Theory and Practice of Free-Electron Lasers

Particle Accelerator School
Day 3

Dinh Nguyen, Steven Russell
& Nathan Moody
Los Alamos National Laboratory

Course Content

Chapter 5
Wigglers

Wigglers

- Maxwell Equations
- Wiggler Designs
  - Pure Permanent Magnet
  - Hybrid
- Wiggler Natural Focusing
- Two-plane Focusing
  - Weak Focusing
  - Strong Focusing
- Tapered Wigglers

Maxwell Equations

Gauss' law for electricity

$$\boxed{\nabla \cdot \mathbf{E} = \frac{\rho}{\varepsilon_0}} \longrightarrow \mathbf{D} = \varepsilon_0 \mathbf{E}$$

Gauss' law for magnetism

$$\boxed{\nabla \cdot \mathbf{B} = 0}$$

Faraday's law

$$\boxed{\nabla \times \mathbf{E} = -\frac{\partial \mathbf{B}}{\partial t}}$$

Ampere's law

$$\boxed{\nabla \times \mathbf{B} = \mu_0 \mathbf{J} + \frac{1}{c^2}\frac{\partial \mathbf{E}}{\partial t}} \longrightarrow \mathbf{B} = \mu_0 \mathbf{H}$$

Maxwell Equations in simple forms

$$\nabla \cdot \mathbf{D} = \rho$$

$$\nabla \cdot \mathbf{B} = 0$$

$$\nabla \times \mathbf{E} = -\frac{\partial \mathbf{B}}{\partial t}$$

$$\nabla \times \mathbf{H} = \mathbf{J} + \frac{\partial \mathbf{D}}{\partial t}$$

Physical Constants

Speed of light	c	2.9979 x 10^8 m/s	$c = \sqrt{\frac{1}{\mu_0 \varepsilon_0}}$
Permeability of vacuum	μ_0	4π x 10^{-7} H/m	
Permittivity of vacuum	ε_0	8.8542 x 10^{-12} F/m	$\varepsilon_0 = \frac{1}{\mu_0 c^2}$
Free space impedance	Z_0	376.73 Ω	$Z_0 = \sqrt{\frac{\mu_0}{\varepsilon_0}} = c\mu_0 = \frac{1}{c\varepsilon_0}$
Electronic charge	e	1.6022 x 10^{-19} C	
Electron mass	m_0	9.1094 x 10^{-31} kg	
Electron rest energy	$m_0 c^2$	0.511 MeV	
Classical electron radius	r_0	2.81794 x 10^{-15} m	$r_0 = \frac{1}{4\pi\varepsilon_0}\frac{e^2}{mc^2}$
Alfven current	I_0	1.7 x 10^4 A	$I_0 = \frac{ec}{r_0} = \frac{1}{4\pi\varepsilon_0}\frac{m_0 c^3}{e}$

Wiggler Designs

- Pure Permanent Magnet (PPM)
  - No power required
  - Highest magnetic field at very short wiggler periods
  - Can accommodate two-plane quadrupole focusing magnets
  - Susceptible to demagnetization
- Hybrid (Permanent Magnet + Iron or Vanadium Permendur)
  - No power required
  - Higher field if the gap-to-period ratio is less than 0.4
  - Magnetic field non-uniformity is reduced if ferromagnetic is saturated
  - Uses more magnet materials than PPM
  - Susceptible to demagnetization
- Electromagnets
  - No risk of demagnetization
  - Lower magnetic field at very short wiggler periods
  - Require external power sources and cooling

Magnet Material Properties

- Rare-earth Magnets
  - $SmCo_5$
  - Sm_2Co_{17}
  - $Nd_2Fe_{14}B$
- Ferromagnetic Materials
  - Iron
  - Vanadium Permendur
- Room-temperature Electromagnets
- Superconducting Electromagnets
  - NbTi
  - NbSn
  - YBCO

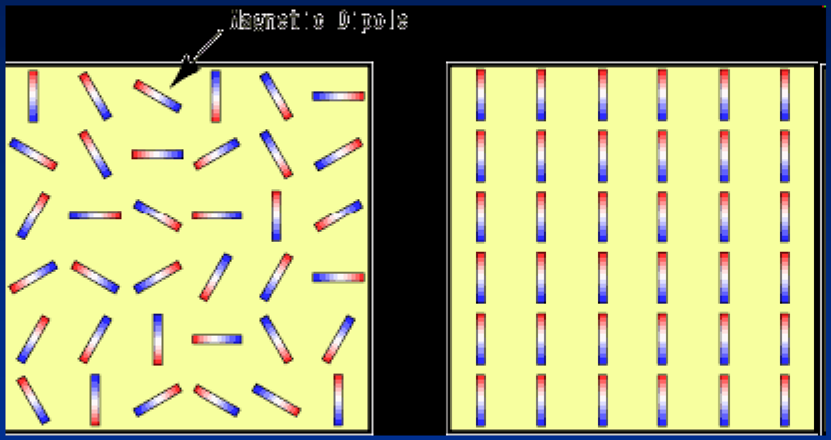

We will not consider electromagnet wigglers here

Magnetization Curves

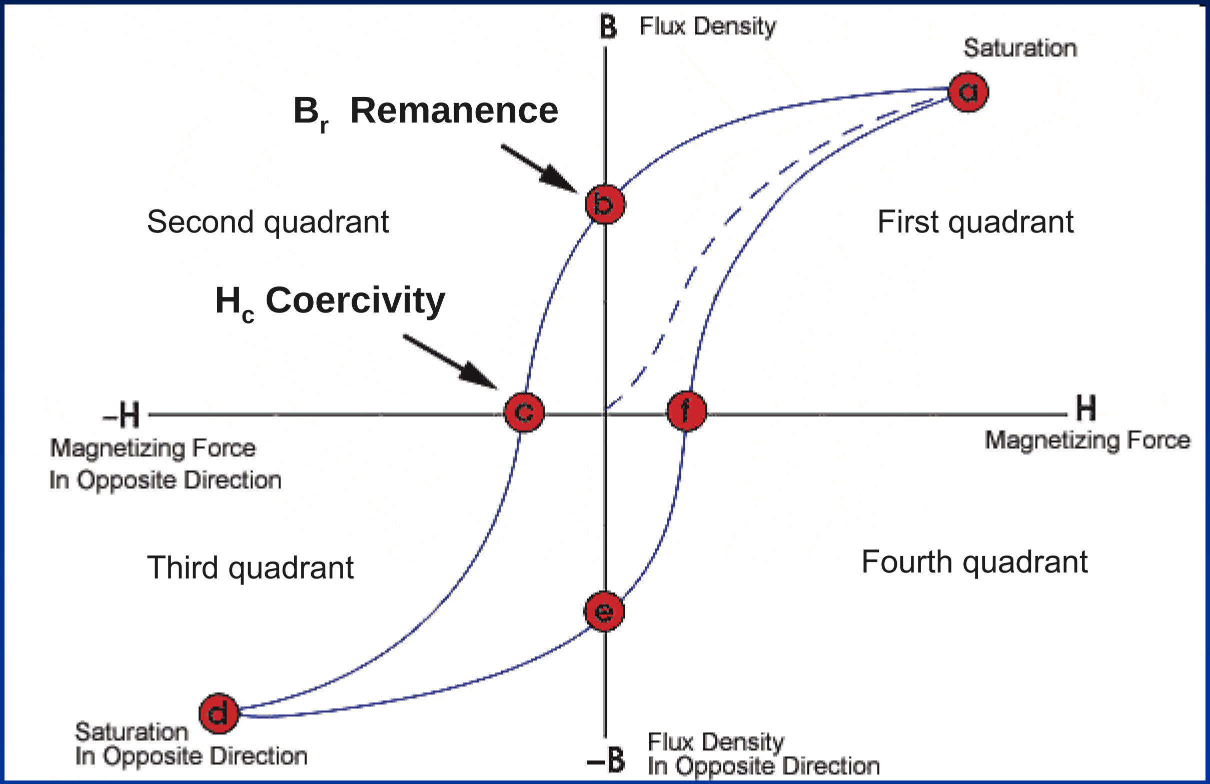

Hysteresis curve starts from the origin and follows the dashed line to saturation (a). After the magnetizing force is removed, the curve moves to (b) and the magnets retains remanent field B_r. Reversing the magnetizing force causes the magnets to be demagnetized beginning at (c) in the 3rd quadrant (danger zone).

Los Alamos NATIONAL LABORATORY EST. 1943

Permanent Magnet Materials

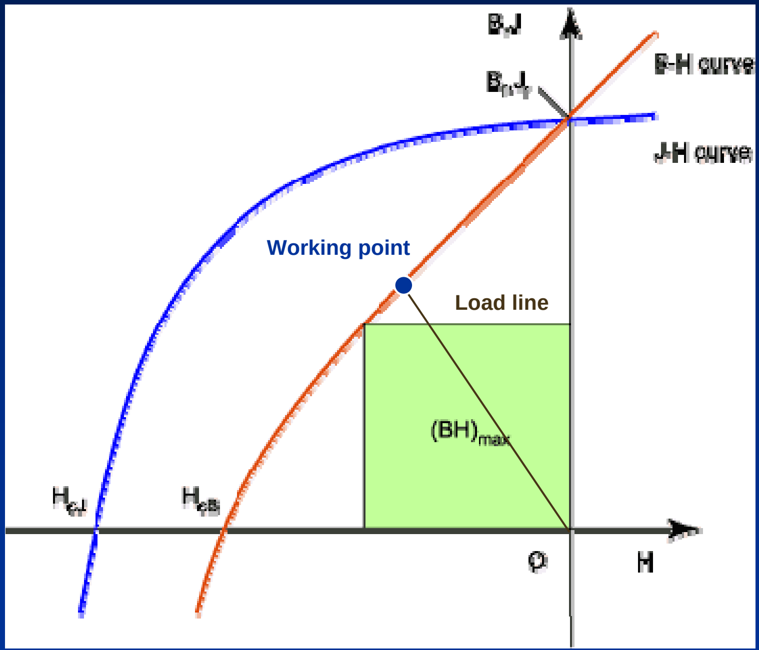

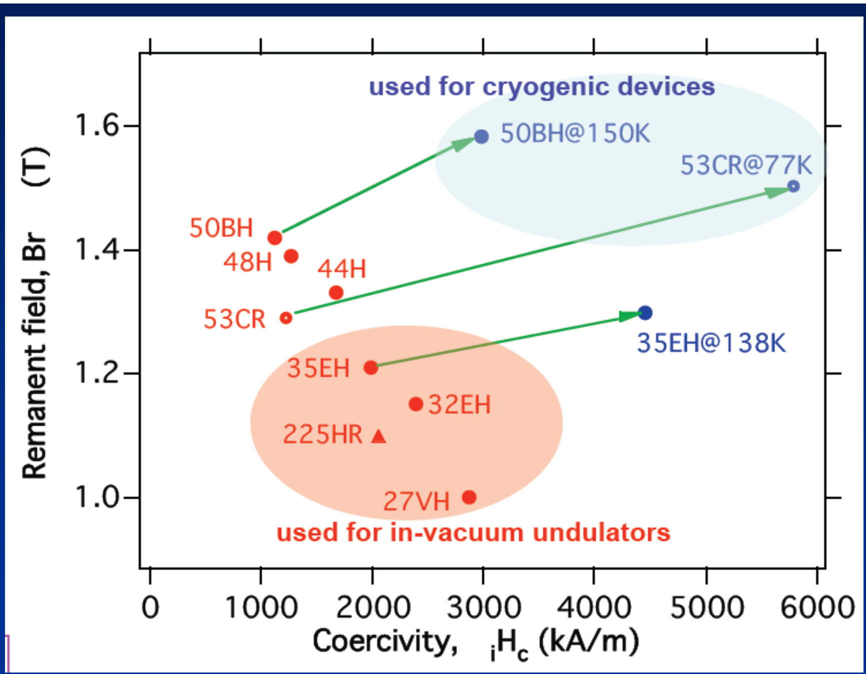

PM Material	$(BH)_{max}$ (kJ/m^3)	Remanence (mT)	B_r Temp Coefficient (% / K)	H_c Coercivity (kA/m)	H_{cB} Temp Coefficient (% / K)	Radiation Hardness
$SmCo_5$	170	800-1000	-0.042	2400	-0.25	High
Sm_2Co_{17}	220	1000-1100	-0.032	2000	-0.19	Medium
NdFeB	300	1100-1400	-0.10	1400	-0.60	Low - Medium

Halbach PPM Wiggler Design

Magnet arrangement

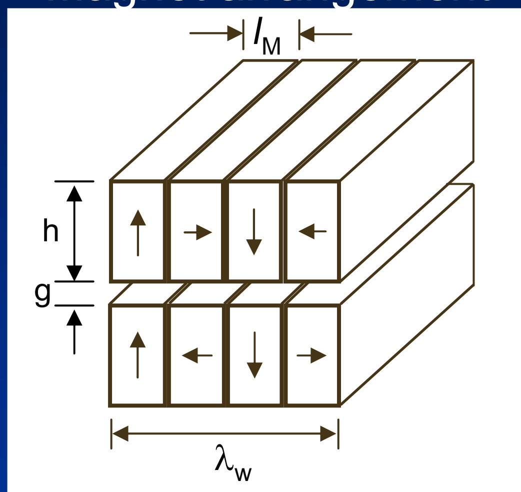

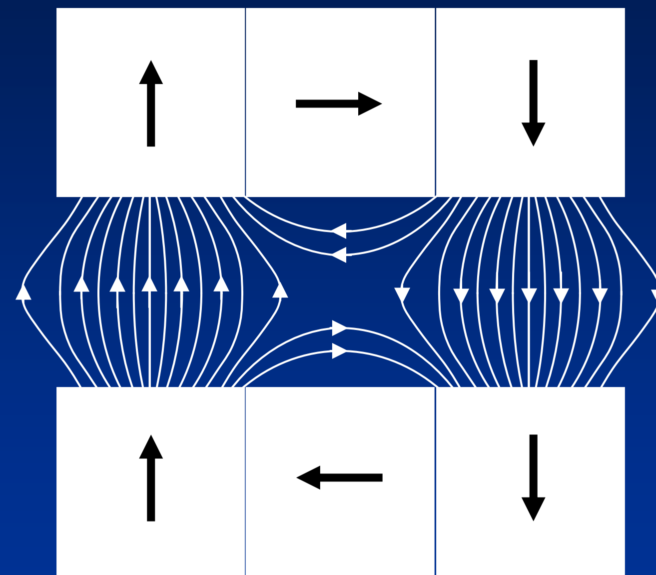

Magnetic field lines

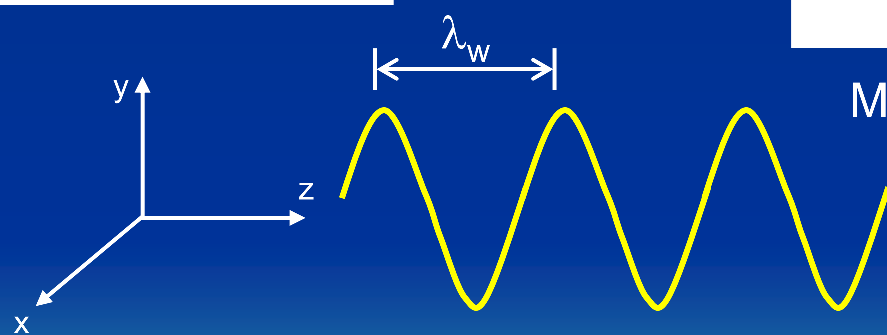

Halbach PPM design uses 4 magnets per period for each jaw (8 on both jaws) to produce a sinusoidal vertical field (B_y) along the z axis.

Peak On-axis Magnetic Field

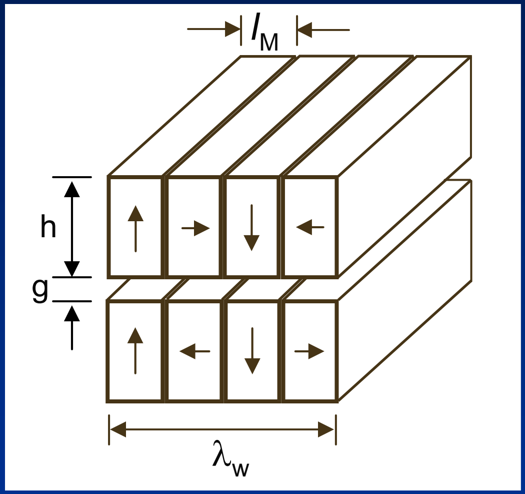

Peak on-axis magnetic field

$$\boxed{B_0 = 2B_r f_M f_H e^{-\pi\frac{g}{\lambda_w}}}$$

$$f_M = \frac{\sin\left(\pi\frac{l_M}{\lambda_w}\right)}{\left(\frac{\pi}{M}\right)}$$

$$f_H = 1 - e^{-\frac{2\pi h}{\lambda_w}}$$

g: Full gap between magnet jaws

B_r: Remanence (a material property)

f_M: Magnet filling factor

l_M: Length of individual magnet (along z)

M: Number of magnets per period (one jaw)

f_H: Magnet height factor

h: Height of individual magnet (along y)

Optimized Halbach design

$$\boxed{B_0 = 1.78 B_r e^{-\frac{\pi \cdot g}{\lambda_w}}}$$

Hybrid Wiggler Designs

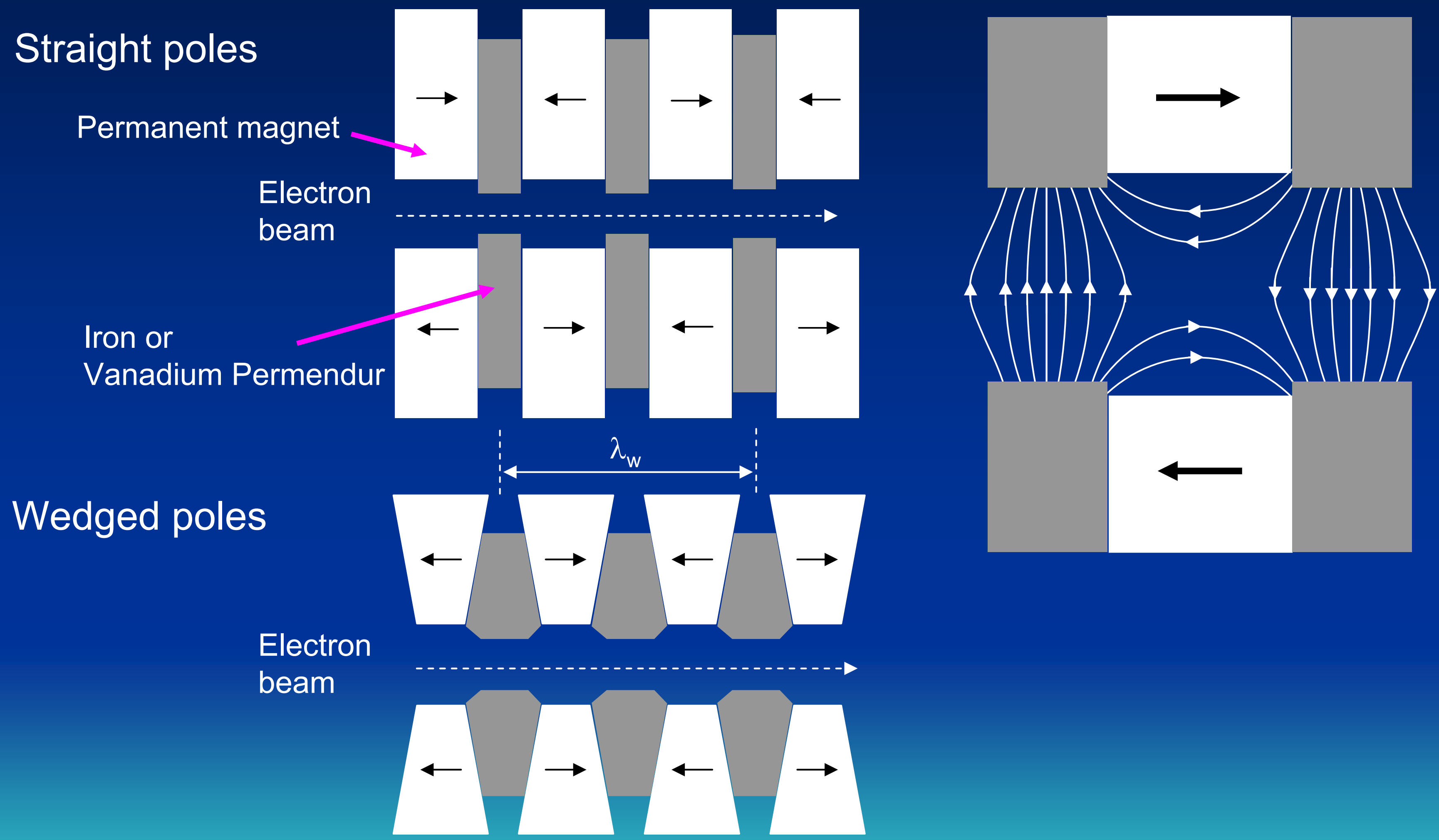

On-axis Field vs Gap-Period Ratio

Empirical formula for peak on-axis field

$$\boxed{B_0 = ae^{-\frac{g}{\lambda_w}\left(b - c\left(\frac{g}{\lambda_w}\right)\right)}}$$

	a	b	c
SmCo	3.33T	5.47	1.8
NdFeB	3.69T	5.07	1.52

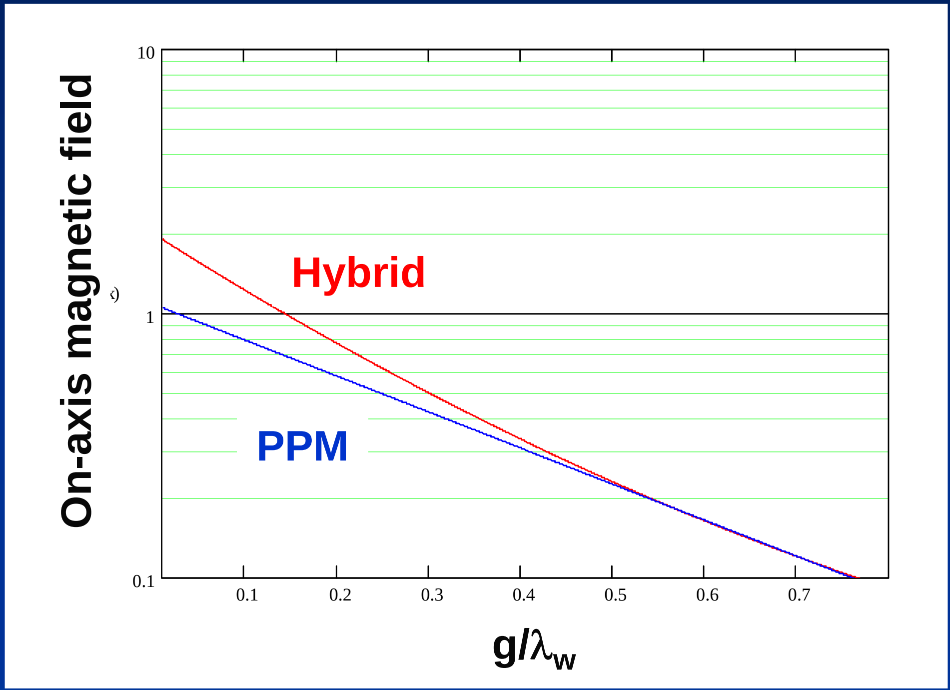

Hybrid wigglers are generally useful for maximizing on-axis field at small gap-to-period ratios. Hybrid wigglers also produce good field uniformity if the ferromagnetic material (iron or Vanadium Permendur) is saturated.

Planar Wiggler Magnetic Field

Planar wiggler with infinite x dimension

$$B_x = 0$$
$$B_y = \hat{y} B_0 \cosh(k_w y)\cos(k_w z)$$
$$B_z = -\hat{z} B_0 \sinh(k_w y)\sin(k_w z)$$

Lorentz force (written as second derivative with respect to z)

$$y'' = \left(\frac{e}{\gamma m_0 c^2}\right)\left(\upsilon_x B_z - \upsilon_z B_x\right)$$

Consider only the first term (B_x = 0).

$$y'' = \left(\frac{e}{\gamma m_0 c}\right) x' B_z$$

Using small $k_w y$ approximation

$$B_z \cong -B_0 k_w y \sin\left(k_w z\right)$$

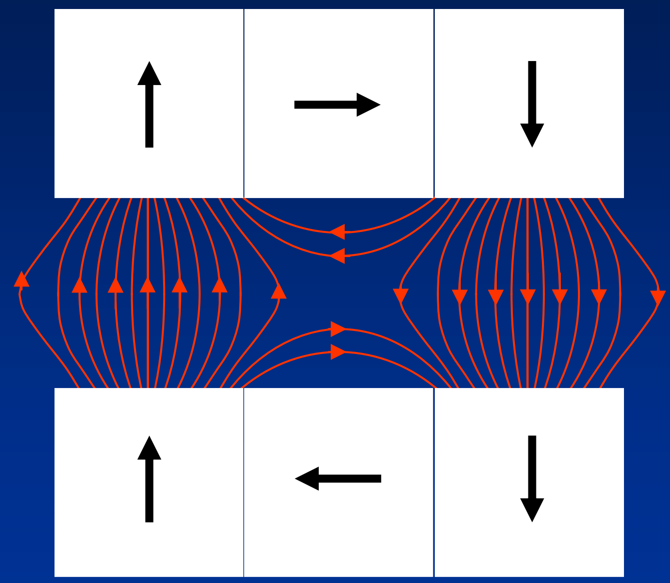

Magnetic field in the y-z plane

Equation of motion in the y direction

$$y'' = -\left(\frac{k_w e B_0}{\gamma m_0 c}\right) x' \sin\left(k_w z\right) y$$

Wiggler Natural Focusing

Expand B_y around y=0

$$B_y = B_0\left[1+\left(k_w y\right)^2\right]\cos\left(k_w z\right)$$

Velocity in x with respect to z

$$x' = -\frac{e}{\gamma k_w m_0 c} B_0\left[1+\left(k_w y\right)^2\right]\sin\left(k_w z\right)$$

Focusing force in the y direction

$$y'' = -\left(\frac{eB_0}{\gamma m_0 c}\right)^2\left[1+\left(k_w y\right)^2\right]\sin^2\left(k_w z\right) y$$

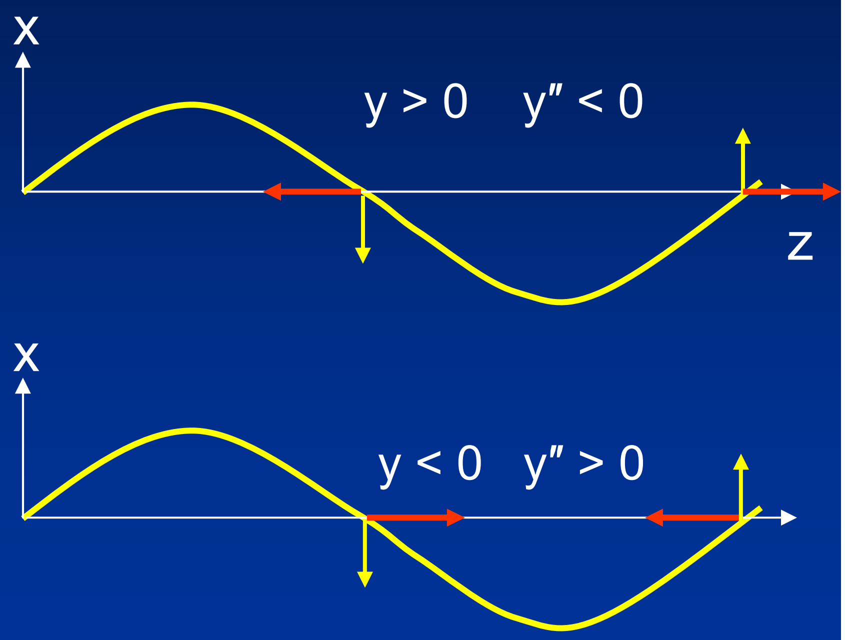

Averaging rapid oscillations (twice the wiggler oscillation) yield the net focusing

$$\boxed{y'' = -\left(\frac{k_w a_w}{\gamma}\right)^2\left[1+\left(k_w y\right)^2\right] y}$$

Vertical and Horizontal Motions

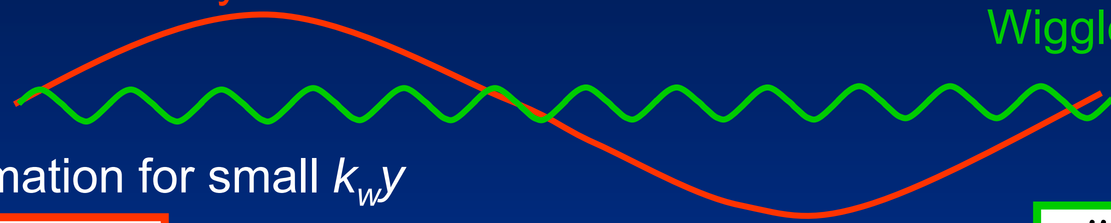

Approximation for small $k_w y$

$$y'' + k_\beta^2 y = 0$$

$$x'' + k_w x = 0$$

$$k_\beta = \frac{eB_0}{\gamma m_0 c} = \frac{k_w a_w}{\sqrt{2}\gamma}$$

Longitudinal velocity (relative to *c*)

$$\beta_\parallel \cong 1 - \frac{1}{2\gamma^2} - \frac{\beta_\perp^2}{2}$$

Transverse velocity (relative to *c*)

$$\beta_\perp^2 = \left(\frac{eB_0}{\gamma k_w m_0 c}\right)^2 \left[1 + \left(k_w y\right)^2\right]$$

Betatron motion is slow, large amplitude motion in the y direction over many wiggler periods due to gradient of B_y along the y direction. The field amplitude is proportional to the square of deviation from the center.

Vertical Envelope Equation

- Vertical envelope equation with emittance

$$\frac{d^2 R_y}{dz^2} + k_\beta^2 R_y = \left(\frac{\varepsilon_{ny}}{\gamma}\right)^2 \frac{1}{R_y^3}$$

- Find matched beam envelope radius by setting $\frac{d^2 R_y}{dz^2}$ to zero

$$R_{y0}^4 = \left(\frac{\varepsilon_{ny}}{\gamma k_\beta}\right)^2$$

$$k_\beta = \frac{k_w a_w}{\sqrt{2}\gamma}$$

Matched beam radius

$$\boxed{R_{y0} = \sqrt{\frac{\sqrt{2}\varepsilon_{ny}}{k_w a_w}}}$$

If the focused electron beam is not the same as the matched beam radius, the *y* envelope will have betatron oscillations along the length of the wiggler.

Wiggler Focusing in a Planar Wiggler

Conventional planar wigglers focus the electron beam only in the y direction. A pair of quadrupoles is used to focus the beam in x and y.

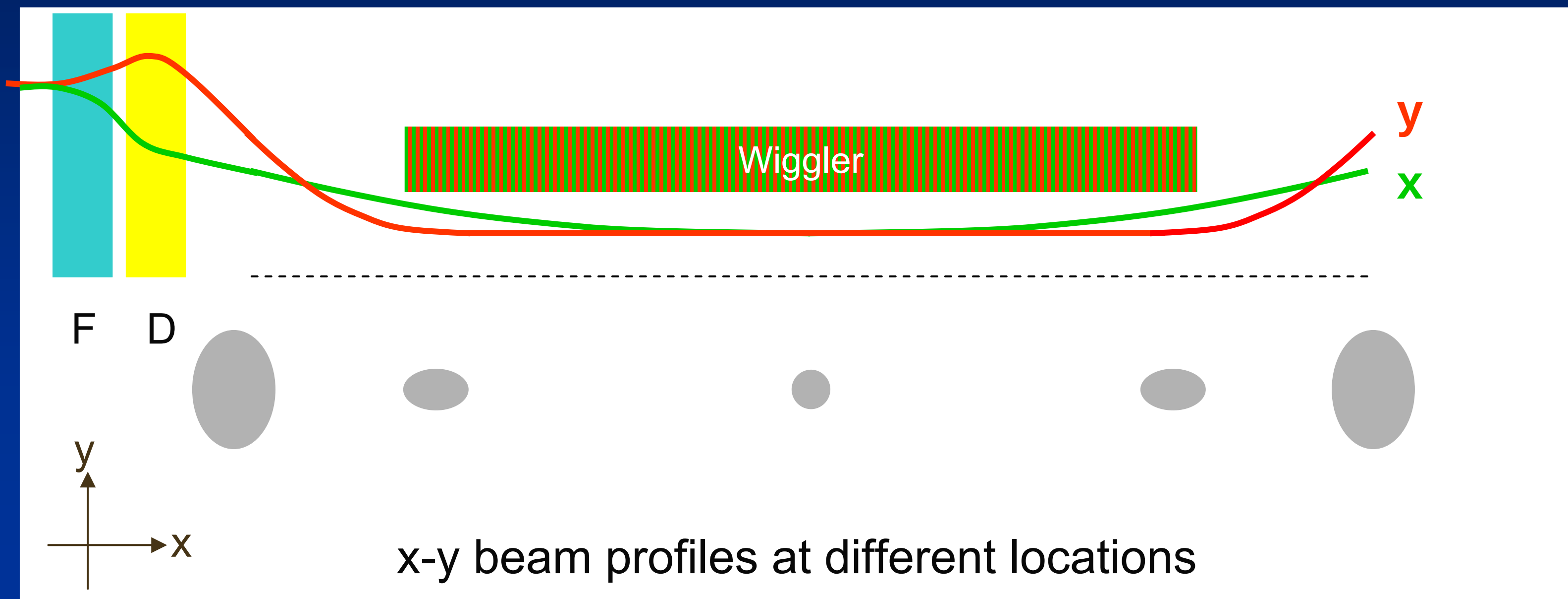

The electron beam is matched into the wiggler with external focusing (by a pair of quadrupole magnets) to form an ellipse (the long axis in x) at the entrance. The matched beam is round only at the center of the wiggler.

Two-plane Weak Focusing

Parabolic Pole Face

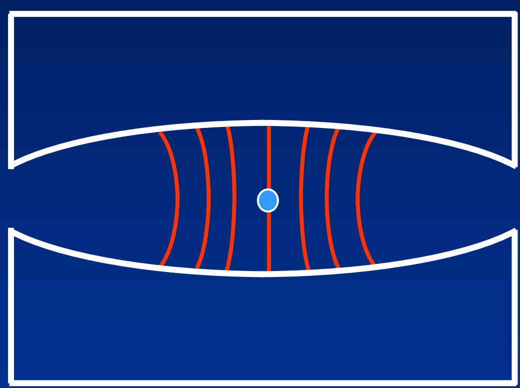

Dual Canted Pole Face

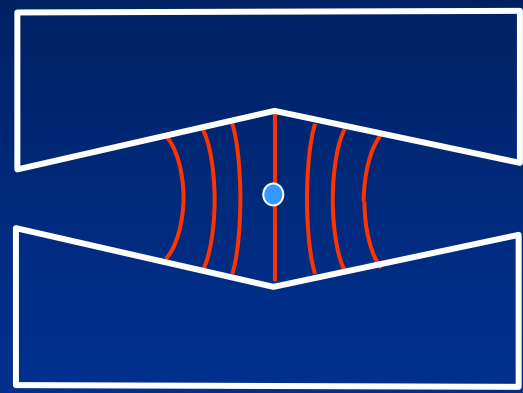

Slotted Pole Face

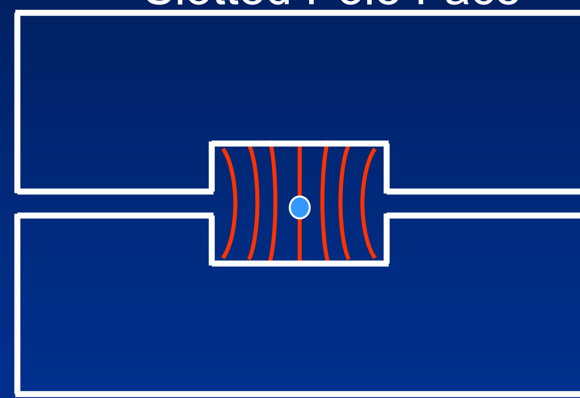

Quadratic x^2 dependence

Approximate x^2 dependence of B_y at the center

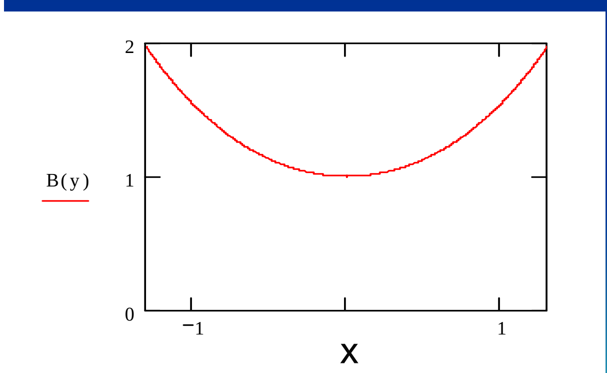

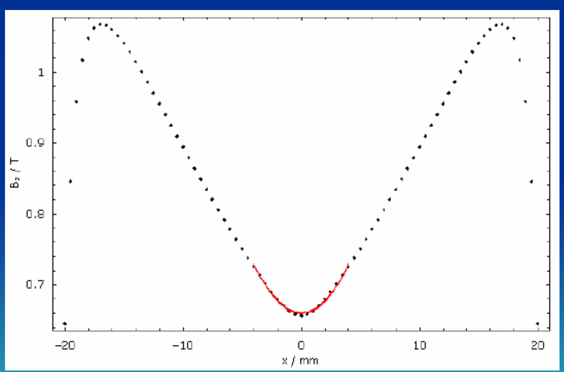

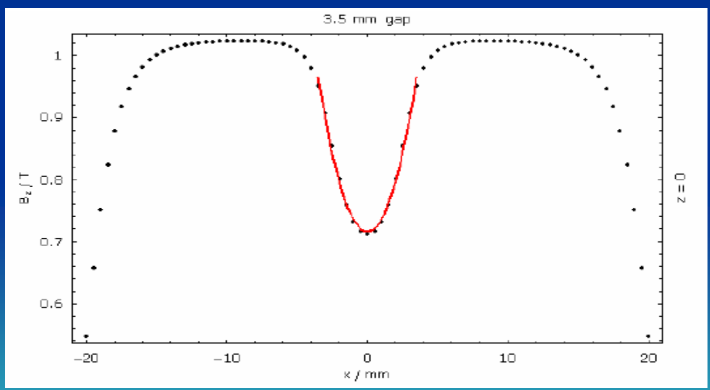

Two-plane Focusing Wigglers

- Wiggler field in a two-plane focusing wiggler

$$B_x = \hat{x} B_0 \frac{k_x}{k_y} \sinh(k_x x) \sinh(k_y y) \cos(k_w z)$$

$$B_y = \hat{y} B_0 \cosh(k_x x) \cosh(k_y y) \cos(k_w z)$$

$$B_z = -\hat{z} B_0 \frac{k_w}{k_y} \cosh(k_x x) \sinh(k_y y) \sin(k_w z)$$

- For small values of x and y (near center) expand *sinh* and *cosh* terms

$$B_x = \hat{y} B_0 k_x^2 xy \cos(k_w z)$$

$$B_y = \hat{y} B_0 \left[1 + \frac{k_x^2 x^2}{2} + \frac{k_y^2 y^2}{2} \right] \cos(k_w z)$$

Matched Beam Radius for Two-Plane Focusing Wigglers

Equations for x and y envelope radii in two-plane focusing wigglers

$$\frac{d^2R_x}{dz^2}+k_x^2R_x=\left(\frac{\varepsilon_{nx}}{\gamma}\right)^2\frac{1}{R_x^3}$$

$$\frac{d^2R_y}{dz^2}+k_y^2R_y=\left(\frac{\varepsilon_{ny}}{\gamma}\right)^2\frac{1}{R_y^3}$$

where

$$k_x^2+k_y^2=k_\beta^2$$

Equal two-plane focusing

$$k_x=k_y=\frac{k_\beta}{\sqrt{2}}$$

Matched beam radii in x and y

$$\boxed{R_{x0}=\sqrt{\frac{2\varepsilon_{nx}}{k_w a_w}}}$$

$$\boxed{R_{y0}=\sqrt{\frac{2\varepsilon_{ny}}{k_w a_w}}}$$

Focusing in y is distributed to focusing in x in natural focusing wigglers.

Strong (Quadrupole) Focusing

Canted Pole Face

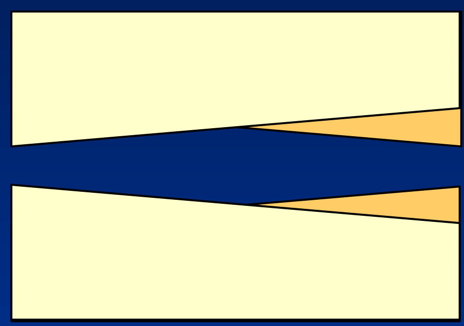

External Quadrupole Magnets

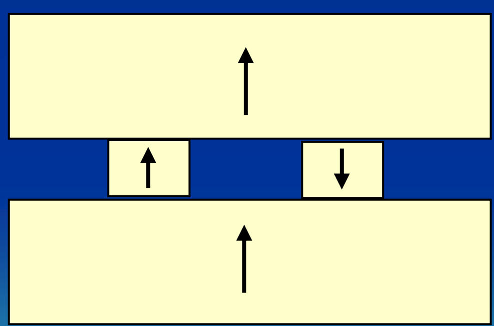

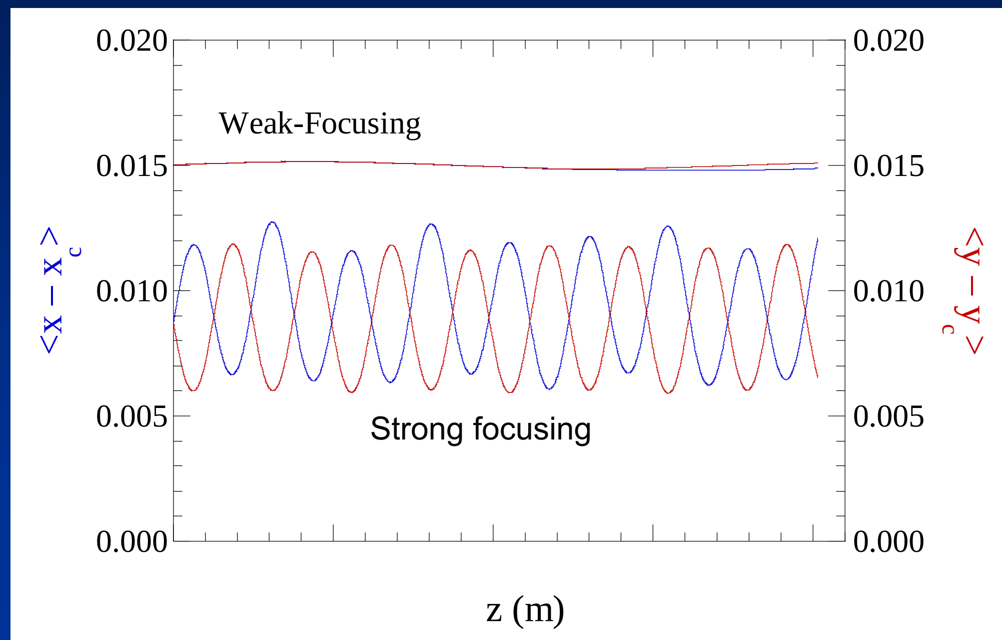

Strong two-plane focusing is used in most x-ray FEL to provide a smaller electron beam in the wiggler (higher gain). However, the longitudinal velocity is modulated by the transverse motion causing periodic dephasing of the FEL interaction.

Wiggler with FODO Focusing

LCLS Wiggler Section

Transfer Matrix

Focusing $$F = \begin{vmatrix} 1 & 0 \\ -1/f & 1 \end{vmatrix}$$

Drift $$O = \begin{vmatrix} 1 & L \\ 0 & 1 \end{vmatrix}$$

Defocusing $$D = \begin{vmatrix} 1 & 0 \\ 1/f & 1 \end{vmatrix}$$

FODO $$M = \begin{vmatrix} 1 & L \\ 0 & 1 \end{vmatrix} \begin{vmatrix} 1 & 0 \\ 1/f & 1 \end{vmatrix} \begin{vmatrix} 1 & L \\ 0 & 1 \end{vmatrix} \begin{vmatrix} 1 & 0 \\ -1/f & 1 \end{vmatrix}$$

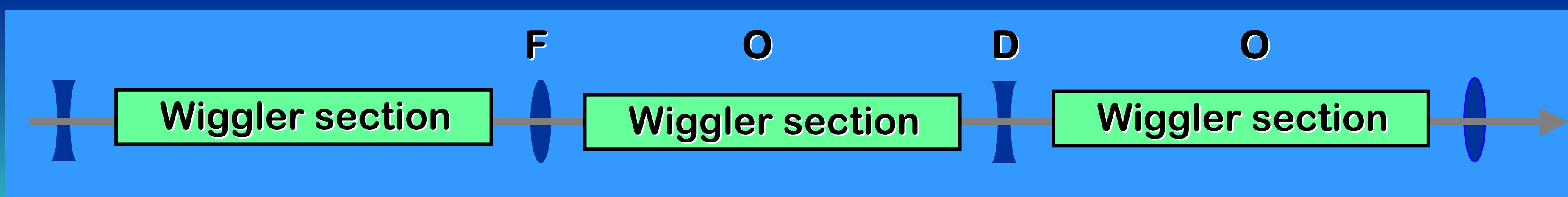

Tapering

As the electron beam's energy changes along the wiggler, the resonance condition is shifted toward lower beam's energy. To maintain resonance, the wiggler period or a_w must be reduced. It is easier to change the wiggler gap g to change the wiggler parameter a_w and thus the resonance energy.

Resonance condition at z_0

$$\lambda = \frac{\lambda_w}{2\gamma^2}\left(1+a_w^2\right)$$

Resonance condition at $z_0 + \Delta z$

$$\lambda = \frac{\lambda_w}{2\left(\gamma-\Delta\gamma\right)^2}\left[1+\left(a_w-\Delta a_w\right)^2\right]$$

Rate of resonance energy change with respect to z

$$\boxed{\frac{d}{dz}\gamma_R^2 = -k_w a_w a_s\left[JJ\right]\sin\phi_R}$$

$$\frac{d}{dz}\left(\frac{\Delta\gamma}{\gamma}\right) = \frac{a_w^2}{1+a_w^2}\frac{d}{dz}\left(\frac{\Delta a_w}{a_w}\right)$$

Different Tapering Methods

- Quadratic taper (black)

$$B_w(z) \approx B_0\left[1-\left(\frac{z-z_0}{L_w}\right)^2\right]$$

- Linear taper (red)

$$B_w(z) = B_0\left[1-s(z-z_0)\right]$$

- Inverse taper (green)

$$B_w(z) = B_0\left[1+s(z-z_0)\right]$$

- Step taper (blue)

$B_w(z) = B_0$ $\quad$ z=0 to z_0

$B_w(z) = B_1$ $\quad$ z=z_0 to z_1

... $\quad$ ....

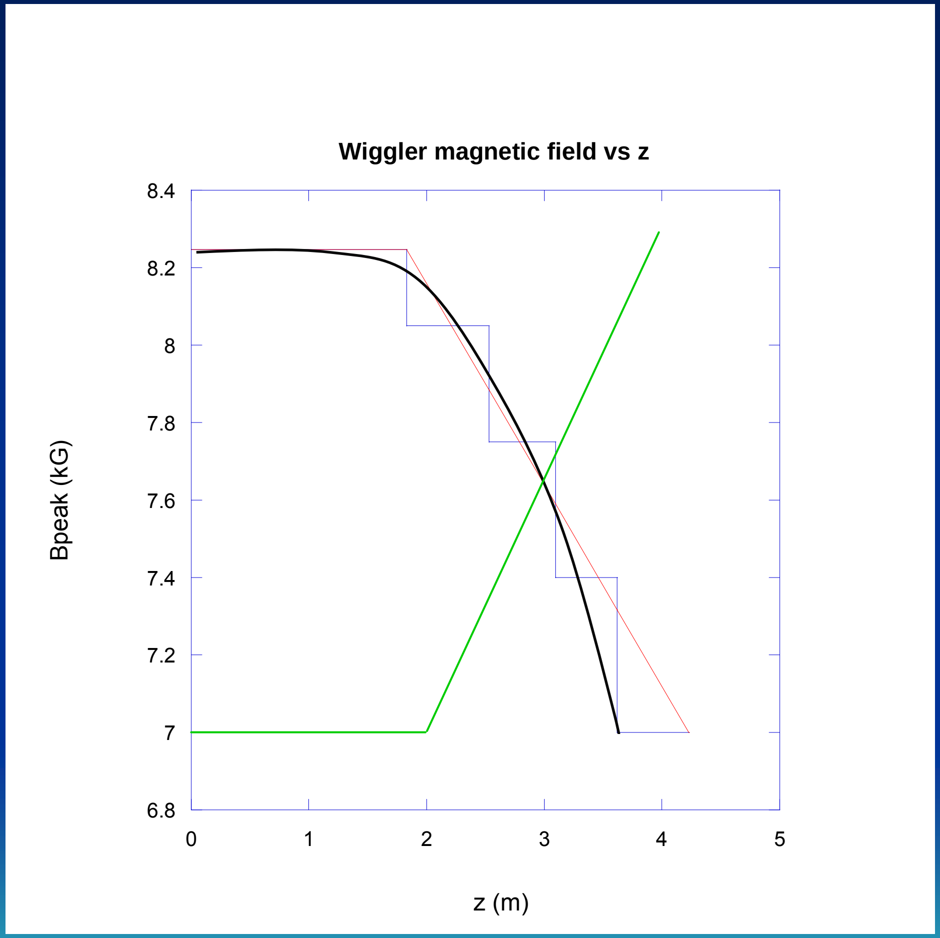

Hamiltonian of Pendulum

$$H = \frac{\nu^2}{2} + V(\zeta)$$

Uniform Wiggler

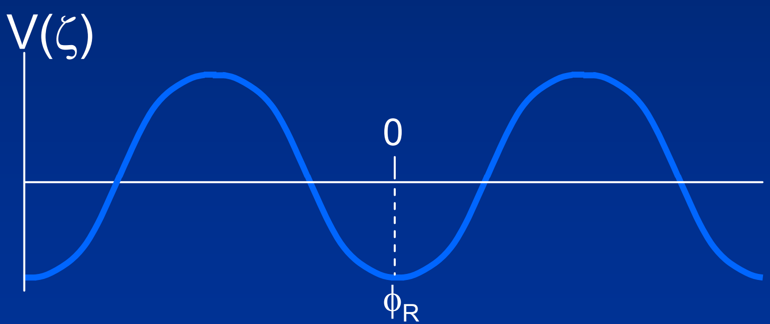

$$V(\zeta) = -|a|\cos\zeta$$

$$\dot{\nu} = -\frac{\partial H}{\partial \zeta} = -|a|\sin\zeta$$

Linearly Tapered Wiggler

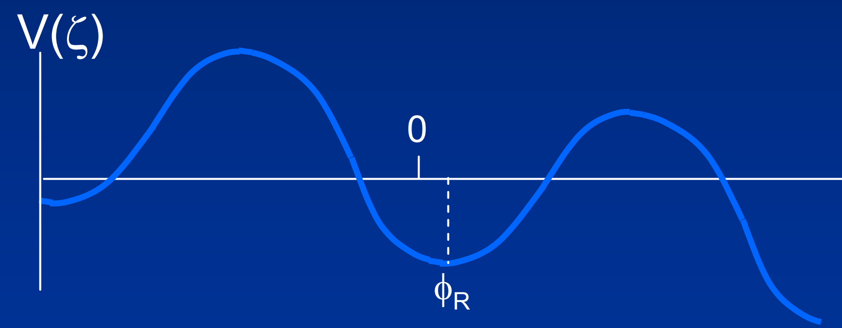

$$V(\zeta) = -|a|\cos(\zeta + \phi_R) + \zeta\sin\phi_R$$

$$\dot{\nu} = -\frac{\partial H}{\partial \zeta} = -|a|\sin(\zeta + \phi_R) + \sin\phi_R$$

Linear Tapered Wiggler

Tapered wiggler pendulum equation

$$\dot{\nu} = |a|\sin(\zeta + \phi_R) + \delta$$

Energy exchange amplitude

$$|a| = \frac{k a_s a_w}{\gamma^2}$$

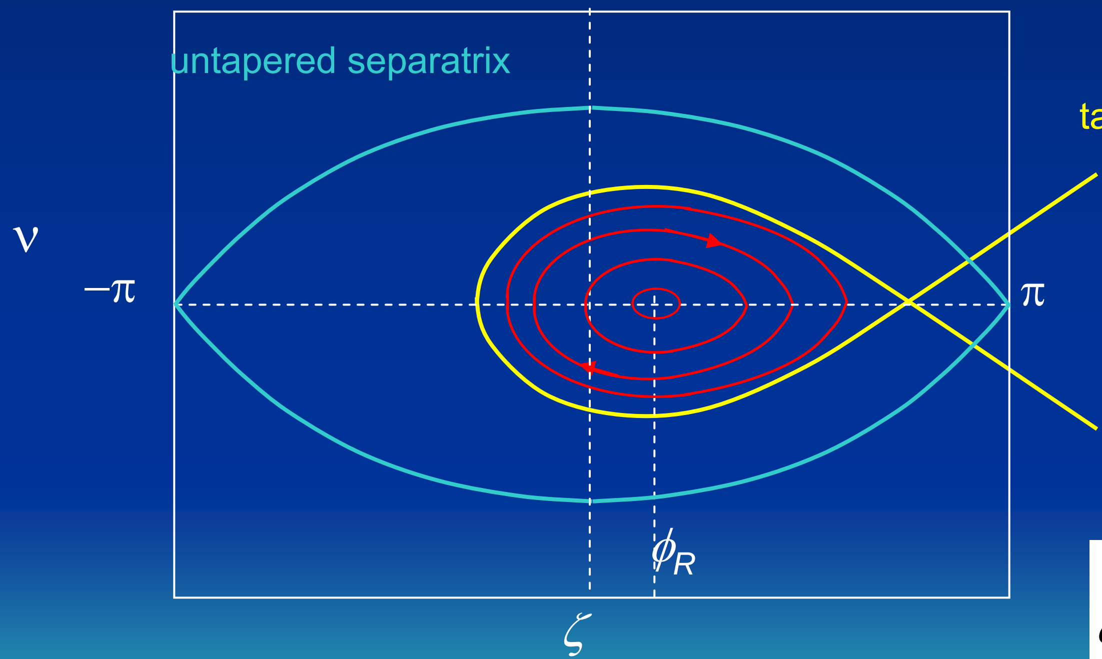

New term in pendulum eq. = phase acceleration

Phase acceleration

$$\delta = \sin\phi_R = \frac{1}{k_w a_s a_w}\frac{d}{dz}\left(\frac{\Delta\gamma}{\gamma_R}\right)$$

Taper Rate & Trapping Fraction

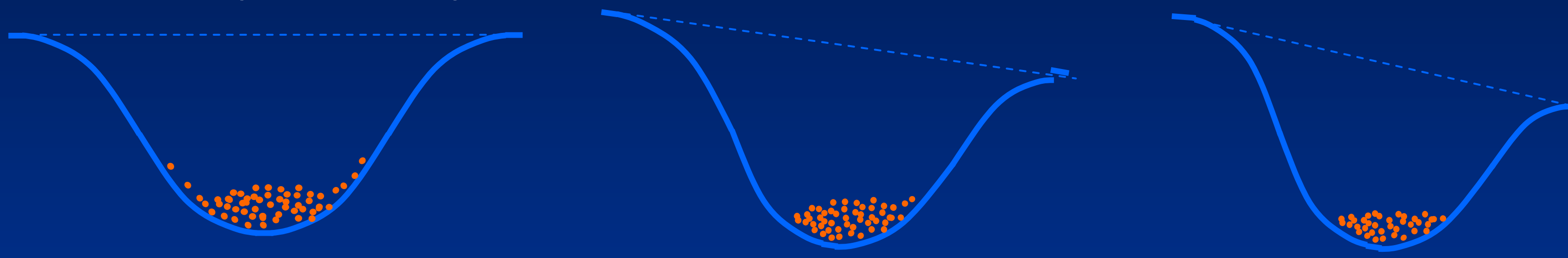

Strong taper rate reduces the phase space area (and particle trapping fraction).

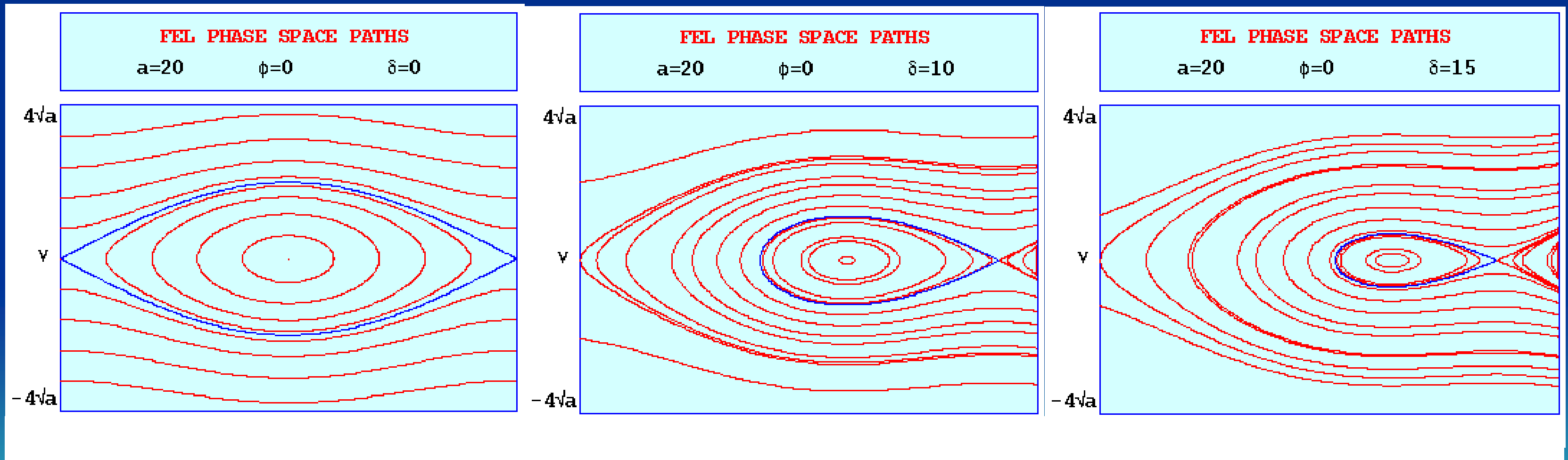

Courtesy of W. Colson

Tapered Wiggler Power Growth

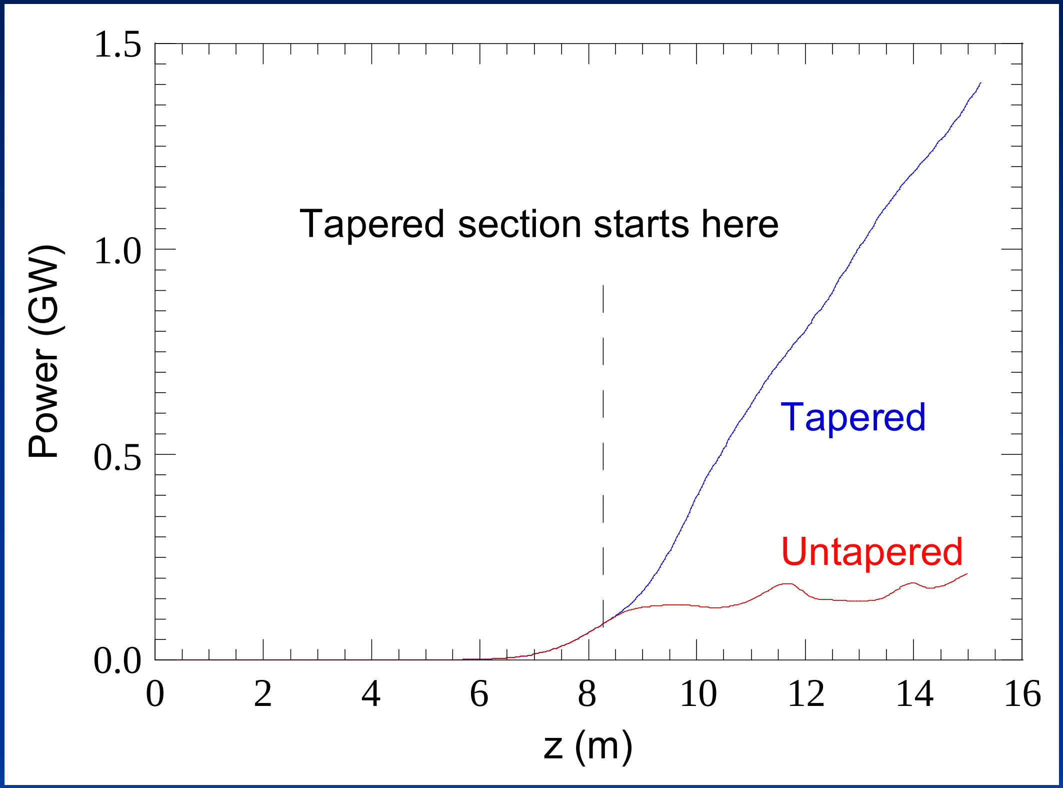

Depending on the trapping fraction and taper length, tapering can increase the power by 2 – 5. The electron trapping fraction decreases with increasing resonant phase and becomes zero if resonant phase = π.

Courtesy of H. Freund

Chapter 6
RF Linear Accelerators

RF Linear Accelerators (Linac)

- Introduction to RF Linac
- Properties of RF Cavities
- Coupled Cavity Linac
- Superconducting RF Linac
- Energy Recovery Linac

Introduction to RF Linac

- Why RF linear accelerators?
- RF linac sub-systems
- Typical performance
- Design choices
    - Travelling-wave vs standing-wave cavities
    - Normal-conducting vs superconducting

RF Linac Pros and Cons

Pros

- Straight linear geometry → No power loss due to synchrotron radiation
- Good beam emittance for short-wavelength FEL
- Can operate at high duty factor to produce high average current
- Can generate short electron bunches to produce high peak current

Cons

- Require complex phase and amplitude controls (Low-level RF)
- Large size
  - Normal-conducting RF: size is dominated by RF generators
  - Superconducting RF: size is dominated by helium cryoplants
- Long, skinny structures not suitable for small packaging

RF linac are the "tried and true" accelerators for short-wavelength FEL.

RF Linac FEL Sub-systems

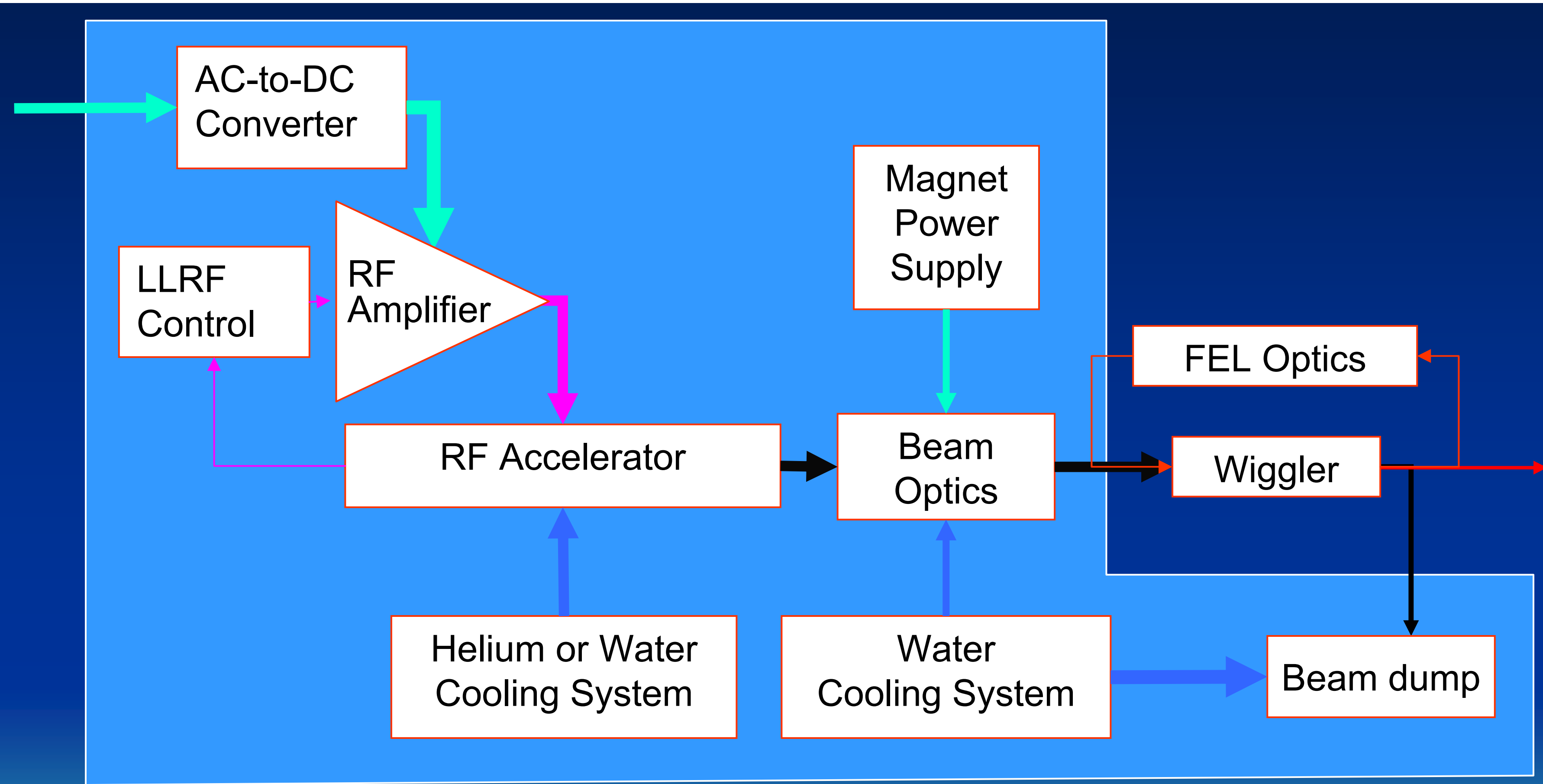

The largest component of an RF linac FEL is the accelerator and its supporting sub-systems. The choice of RF linac determines the FEL performance.

Power Flow in an RF Linac FEL

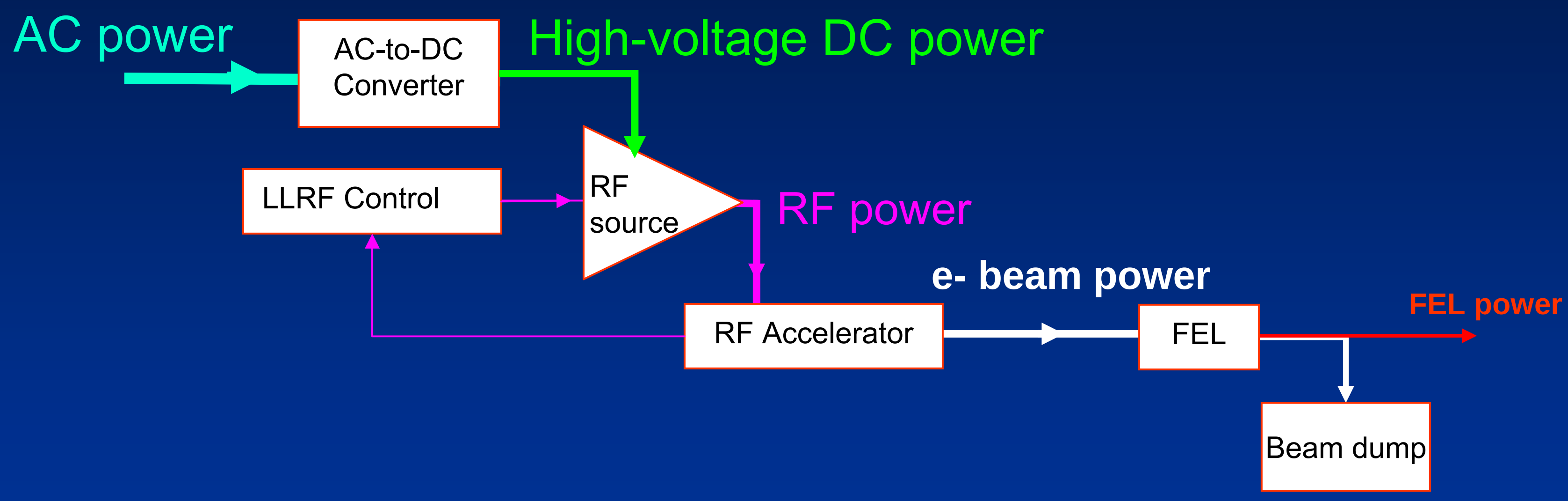

Power is transferred from wall AC → high voltage DC → RF → electron beams → FEL. The wall-plug efficiency, without energy recovery, is the product of efficiencies of all the conversion steps. RF-linac driven FEL without energy recovery have wall-plug efficiency much less than 1%. What we gain is substantial increase in phase space density, i.e., number of photons divided by phase space volume (product of area, solid angle, time and bandwidth).

RF Linac Typical Parameters

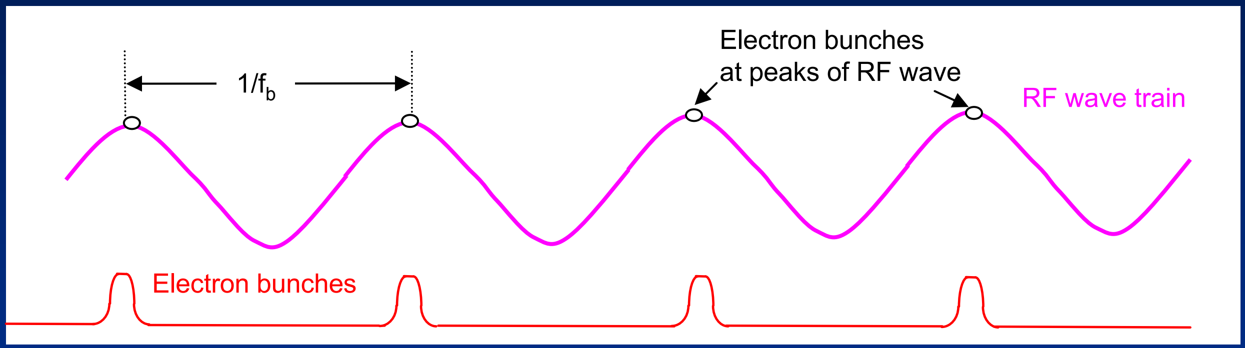

Typical RF frequency	325, 500, 805, 1300, 1500 & 2856 MHz
Electron charge	0.1 – 10 nC
Electron peak current	1 – 100 A
Electron average current	1 μA – 10 mA
Accelerating gradients	
Pulsed normal-conducting	30 – 50 MV/m
cw normal-conducting	2 MV/m
cw superconducting	15 – 35 MV/m

Travelling vs Standing-wave

- In a travelling-wave linac, the RF wave travels from one end of the linac to the other end and into a match load at group velocity $v_g < c$. The phase velocity is slowed down (loaded) by irises to c ($v_p = c$). Electrons are injected at the peak of the RF and co-propagate with the wave in the linac.

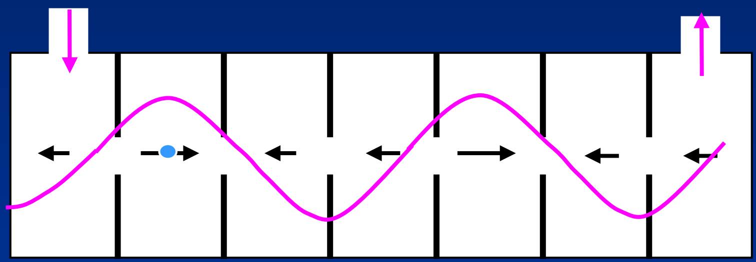

Cavity fill time in TW cavity

$$t_{fill} = \frac{L_c}{\upsilon_g}$$

- In a standing-wave linac, RF power is fed into all the cells at once but the cavity field builds up slowly over time due to the high Q of the cavity. Electrons are usually injected when the cavity power reaches steady state. The phase velocity is zero; however, as the wave reverses periodically, the particles are synchronous only at a few specific values of phase advance.

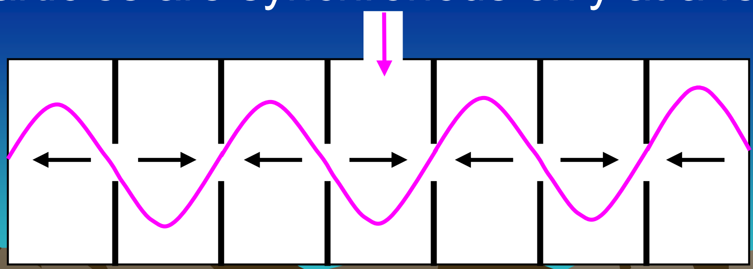

Cavity fill time in SW cavity

$$t_{fill} = \frac{2Q}{\omega}$$

Superconducting vs Normal-Conduting

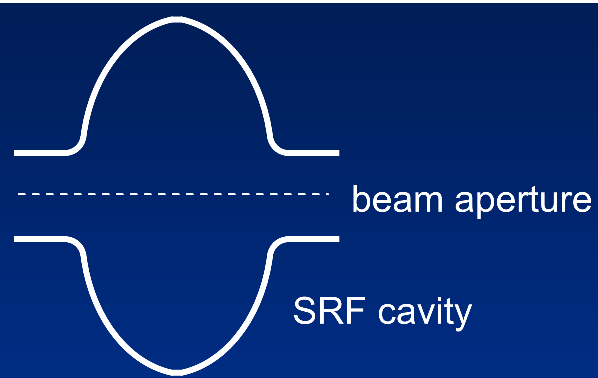

Superconducting

- Niobium at 2K or 4.2K (helium BP)
- Elliptical cavities
- R_s ~ 15 nΩ
- Unloaded Q ~ 2 x 10^{10}
- RF consumption ~ 50 W/m
- Power to remove heat ~ 1 kW/W
- Electricity use ~ 50 kW/m
- Large aperture, small wake field

Normal-conducting

- Copper at room temperature
- Cavities with nose cones
- R_s ~ 10 mΩ
- Unloaded Q ~ 3 x 10^4
- RF consumption ~ 10 MW/m
- Power to remove heat ~ 1 W/W
- Electricity use ~ 10 MW/m
- Small aperture, large wake field

Properties of RF Cavities

- Wave Equations
- Waveguide Modes
- Cavity Modes
- Dispersion Diagram
- Stored Energy, Cavity Q and Losses
- Equivalent Circuits
- Shunt Impedance
- Transit Time
- Gradients, E_0T and ZT^2
- RF Coupling

Wave Equations

Faraday's law

$$\nabla \times \mathbf{E} = -\frac{\partial \mathbf{B}}{\partial t}$$

Ampere's law in vacuum (J = 0)

$$\nabla \times \mathbf{B} = \frac{1}{c^2}\frac{\partial \mathbf{E}}{\partial t}$$

Combine the above 1st–order equations to obtain 2nd–order equations

$$\nabla^2 \mathbf{E} - \frac{1}{c^2}\frac{\partial^2 \mathbf{E}}{\partial t^2} = 0 \qquad \nabla^2 \mathbf{B} - \frac{1}{c^2}\frac{\partial^2 \mathbf{B}}{\partial t^2} = 0$$

Wave equations in cylindrical coordinates

$$\boxed{\left(\frac{\partial^2}{\partial z^2} + \frac{1}{r}\frac{\partial}{\partial r} + \frac{\partial^2}{\partial r^2} - \frac{1}{c^2}\frac{\partial^2}{\partial t^2}\right)\begin{pmatrix}\mathbf{E}\\ \mathbf{B}\end{pmatrix} = 0}$$

Boundary conditions for conducting surfaces:

- $E_{\parallel}$ and $B_{\perp}$ are zero
- $E_{\perp}$ is proportional to surface charge density
- $B_{\parallel}$ is proportional to current density

$$\mathbf{n} \times \mathbf{E} = 0 \qquad \mathbf{n} \cdot \mathbf{B} = 0$$

$$\mathbf{n} \cdot \mathbf{E} = \frac{\Sigma}{\varepsilon_0} \qquad \mathbf{n} \times \mathbf{B} = \mu_0 \mathbf{K}$$

Waveguide Modes

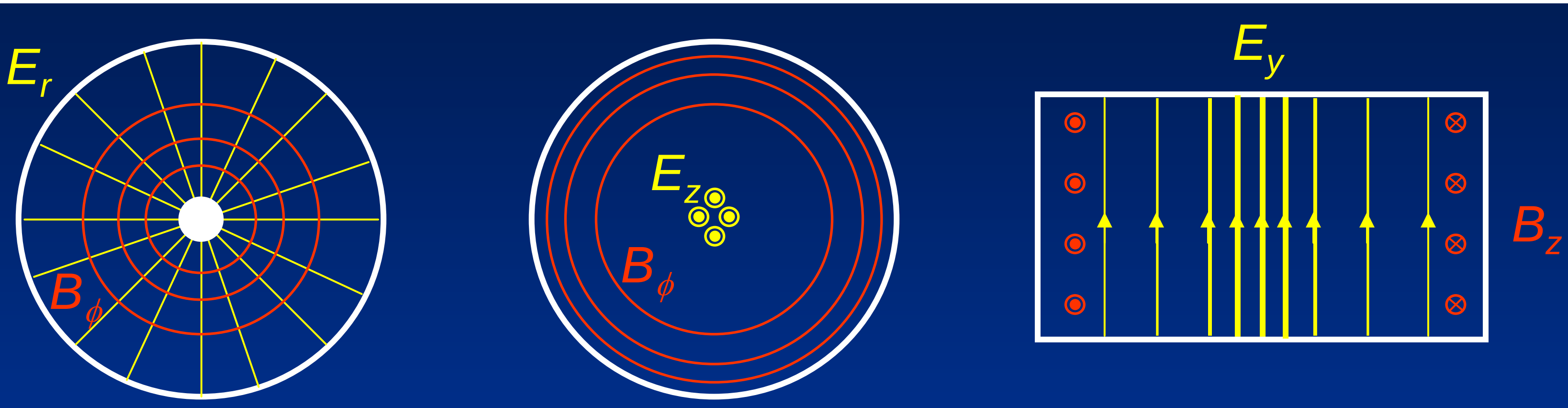

TEM TM TE

TEM (transverse electric and magnetic) modes have no axial field. TEM modes in coaxial transmission lines are used for power transmission at low frequencies. TEM modes are also used for acceleration in $\lambda/2$ and $\lambda/4$ cavities.

TM (transverse magnetic) modes have axial electric field. The lowest TM mode of a pillbox cavity, TM_{010} mode, is used for particle acceleration.

TE (transverse electric) modes have axial magnetic field. The lowest mode in rectangular waveguides, TE_{10} mode, is used for RF power transmission. The width of a rectangular waveguide is one-half the cut-off wavelength.

Waves in Cylindrical Waveguide

Choose solution of the form $E_z(r,z,t) = E_0\,\mathrm{R}(r)e^{ikz}e^{-i\omega t}$

Wave equation becomes Bessel differential equation

$$\frac{\partial^2 R}{\partial r^2} + \frac{1}{r}\frac{\partial R}{\partial r} + \underbrace{\left(\frac{\omega^2}{c^2} - k^2\right)}_{K^2} R = 0$$

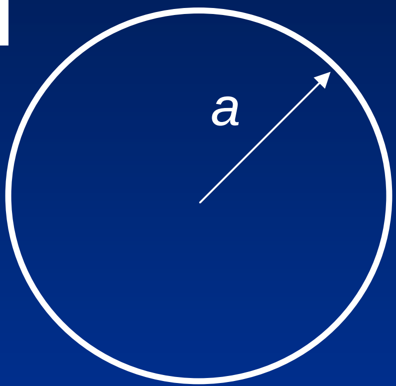

For negative value of K^2, the waves cannot propagate (cut off). The cut-off wavenumber is $\boxed{k_c = \frac{2.405}{a}}$

For positive values of K^2, solutions exist in the form of J_m (electric field) and J'_m (magnetic field) Bessel functions. The zeros of the Bessel functions correspond to solutions of the above differential equation.

$$\boxed{\begin{aligned} E_z(r,\phi,t) &= E_0 J_m(k_{mn}r)\cos(m\phi)e^{i\omega t} \\ B_\phi(r,z,t) &= -iB_0 J'_m(k_{mn}r)\cos(m\phi)e^{i\omega t} \end{aligned}}$$

TM Modes in Cylindrical Waveguides

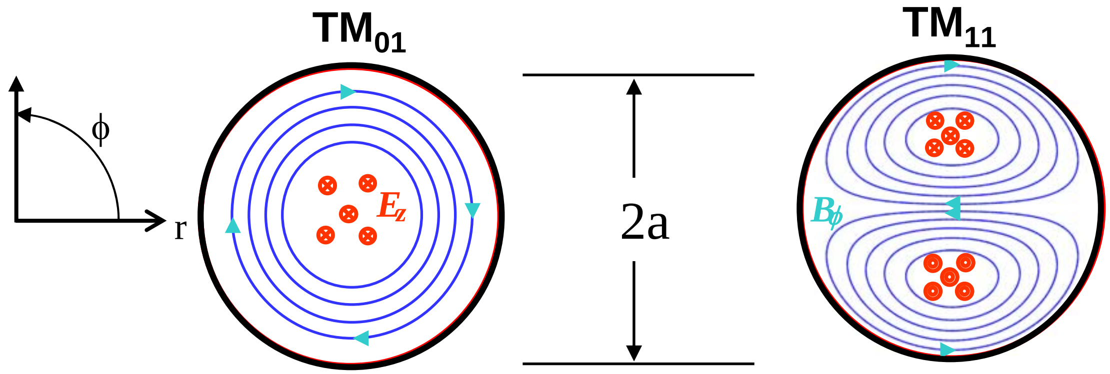

First index = number of full period variations in ϕ
Second index = number of nodes of electric field in the radial direction (excluding the node at r = 0)

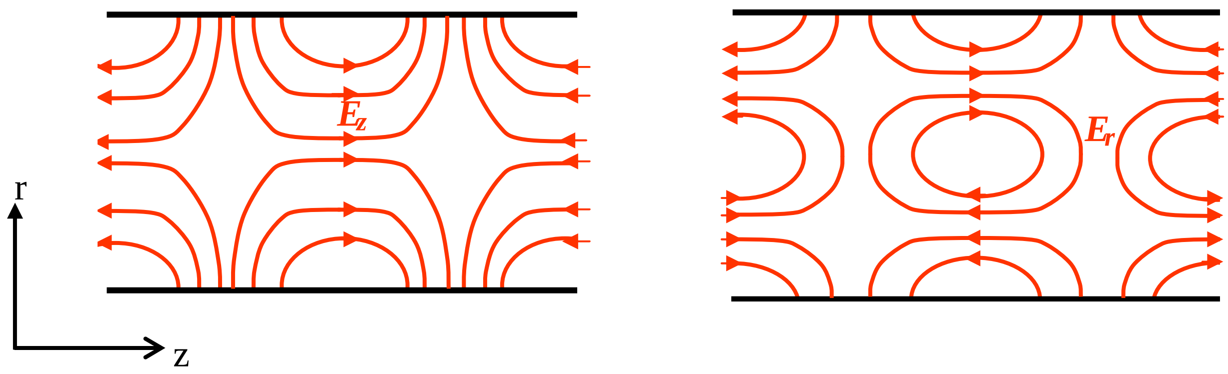

Dispersion Diagram for Unloaded Waveguides

Dispersion relation

$$\frac{\omega^2}{c^2} = k_c^2 + k^2$$

Cut-off frequency

$$\omega_c = k_c c$$

Slope = phase velocity > c

$$v_p = \frac{c}{\sqrt{1-\left(\frac{\omega_c}{\omega}\right)^2}}$$

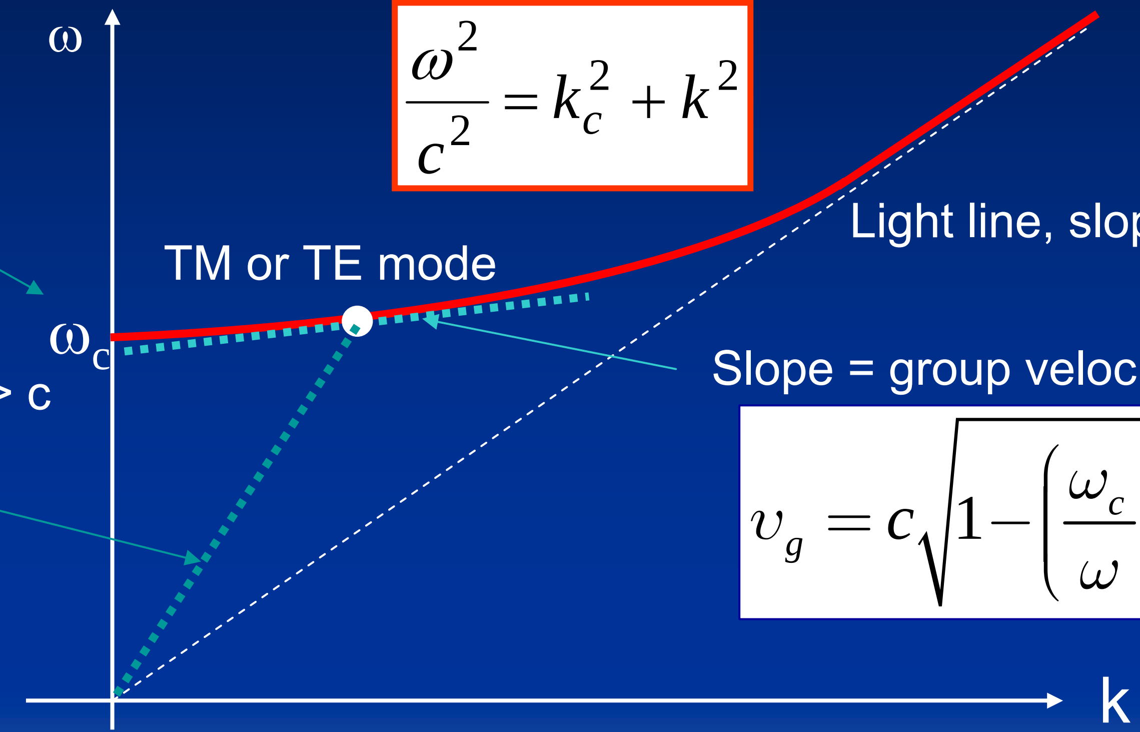

Slope = group velocity < c

$$v_g = c\sqrt{1-\left(\frac{\omega_c}{\omega}\right)^2}$$

Phase velocity of EM wave is faster than the speed of light in uniform waveguides.
Electrons see a time-varying electric field that averages to 0 (no net acceleration).

Dispersion Diagram for Periodically Loaded Waveguides

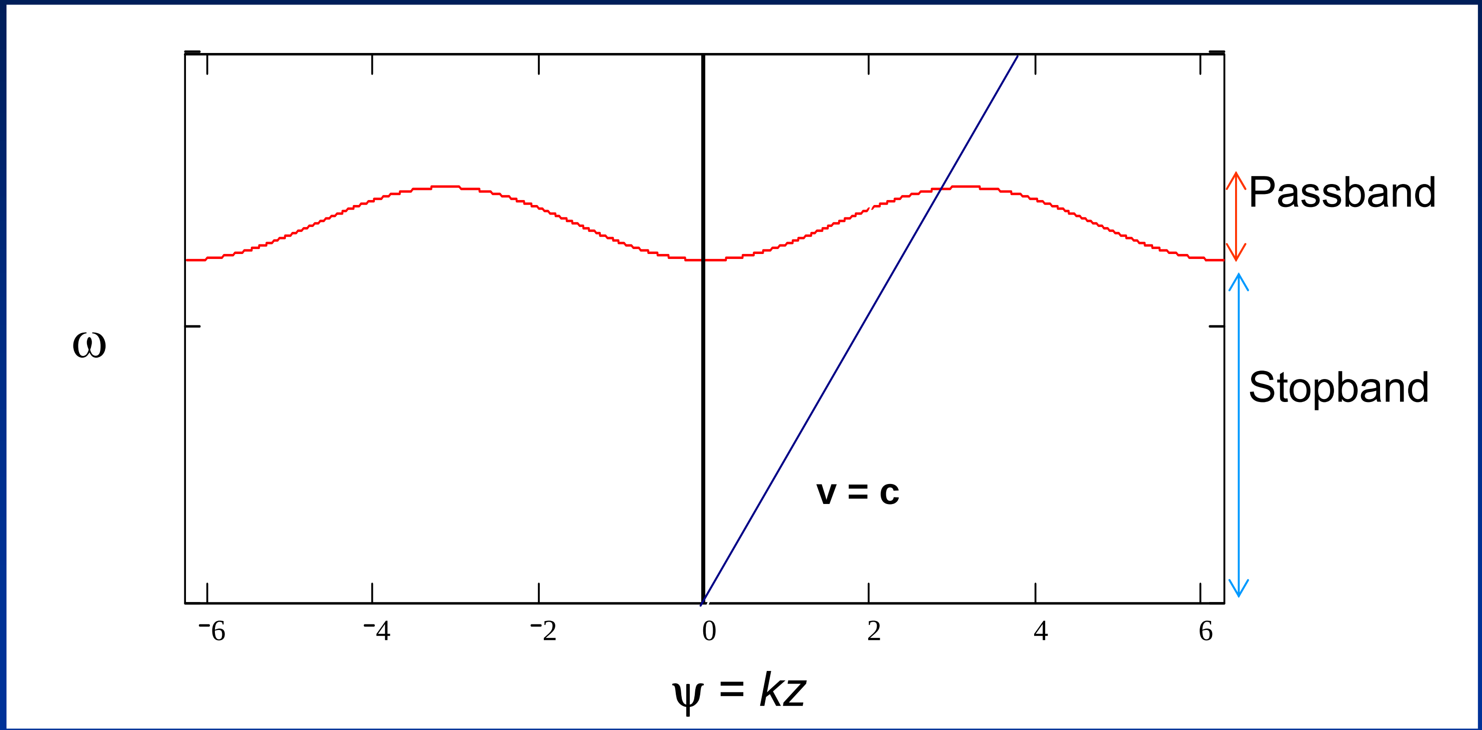

The RF phase velocity is reduced by "**loading**" the structure with periodic structures. The dispersion curve intercepts the light line at the synchronous phase advance. For travelling wave cavities, the typical phase advance is $2\pi/3$. The most common phase advance for standing wave cavities is π.

Pillbox Cavity

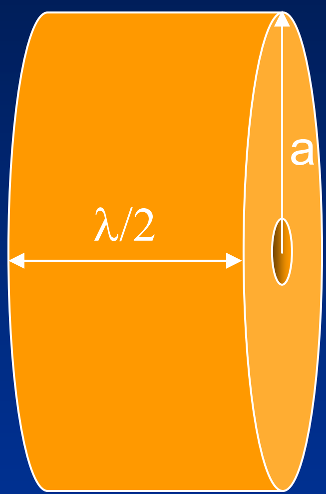

$$\omega = 2.405\frac{c}{a}$$

$$f = \frac{11.475GHz}{(a/cm)}$$

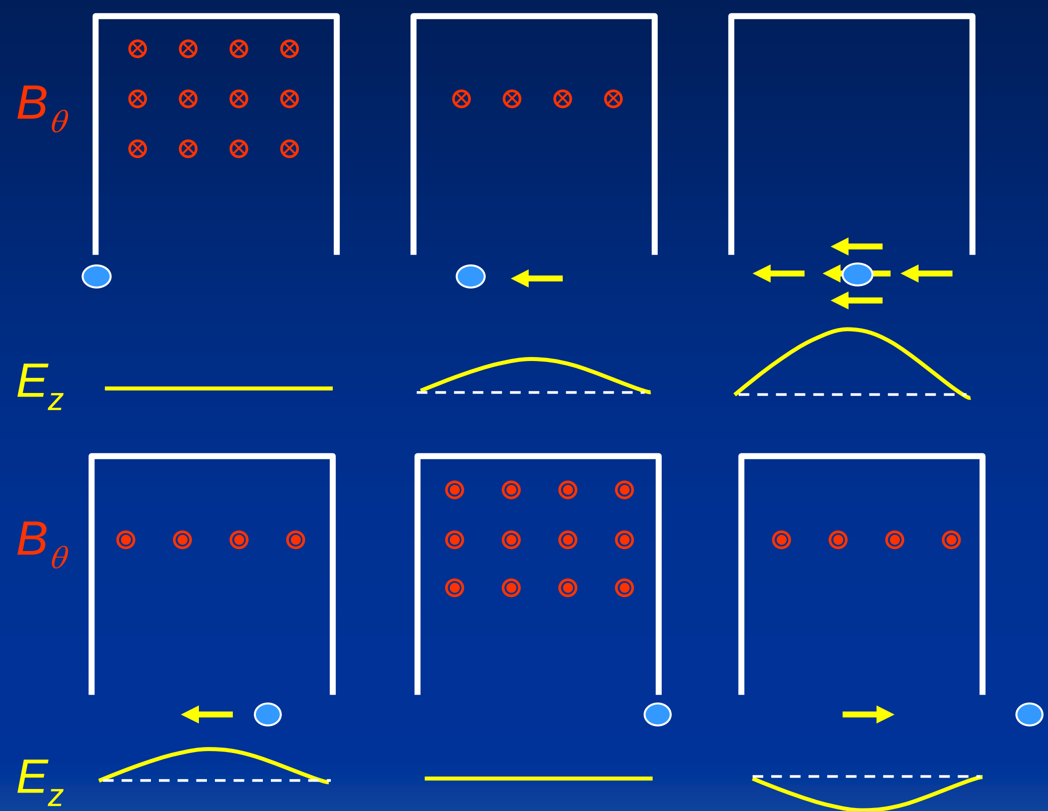

TM$_{010}$ is the accelerating cavity mode. The 3rd index refers to number of half-period variations in the z direction. The resonance frequency of a pillbox is inversely proportional to its radius. The cell length is typically one-half the RF wavelength. Electrons enter and exit the cell at zero field and see maximum field in the center.

TM_{010} Mode

TM_{010} has axial (along z) electric field.

$$E_z(r,z,t) = E_0 J_0(k_c r)\cos(kz - \omega t)$$

$$B_\phi(r,z,t) = \frac{E_0}{c}\frac{\omega}{\omega_c} J_1(k_c r)\sin(kz - \omega t)$$

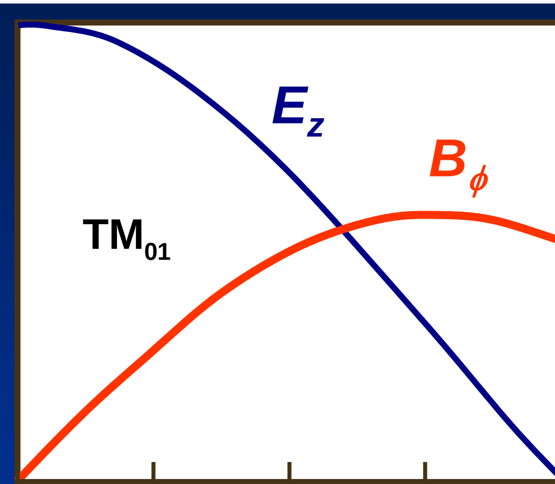

$r = 0$ $r = a$

Poynting vector

$$S = E \times H^*$$

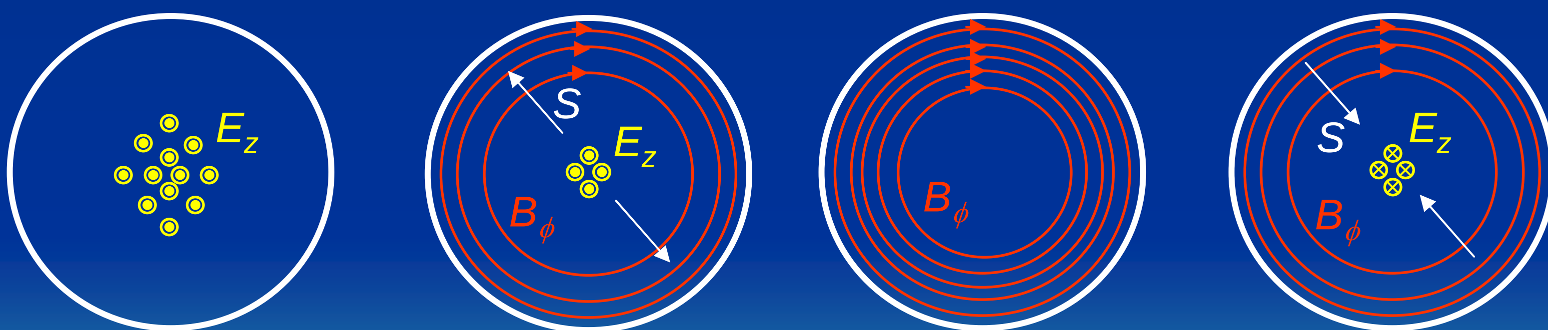

Axial electric field is peaked on axis and decays to zero at the wall.
Azimuthal magnetic field is peaked at ~0.75*a* and does not vanish at *r* = *a*.
The stored energy goes back and forth between electric and magnetic fields.

Surface Resistance

Normal conductor surface resistance

$$R_S = \frac{1}{\sigma\delta}$$

Electrical conductivity

Skin depth

$$\delta = \sqrt{\frac{2}{\omega_0 \mu_0 \sigma}}$$

Superconductor surface resistance

$$R_S = R_{BCS} + R_{res}$$

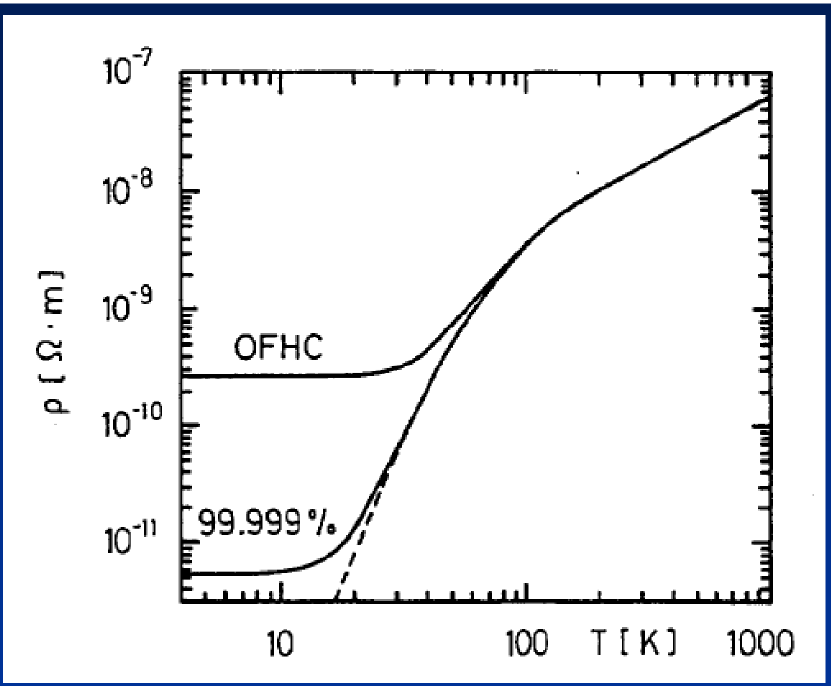

For normal conductors, resistance is caused by collisions with impurities, lattice defects, or ions due to their thermal motions. Superconductors have two components to surface resistance: BCS resistance and residual resistance.

RT copper at 1.3 GHz	σ = 5.8 x 10^7 A/(V-m)	δ = 1.7 μ	R_s = 10 mΩ
2K niobium at 1.3 GHz	R_{BCS} = 7 nΩ	R_{res} = 8 nΩ	R_s = 15 nΩ

Stored Energy, Loss and Cavity Q

Stored energy

$$U = \frac{\mu_0}{2} \int |\mathbf{H}|^2 dV$$

Ohmic loss

$$P_l = \frac{R_S}{2} \int |\mathbf{H}|^2 dS$$

Cavity unloaded Q is the ratio of stored energy to power loss per cycle. Cavity Q is a function of both geometry and material (surface resistance). The geometric factor G is measured in ohm. For a given G, the lower the surface resistance, the higher the cavity Q.

Cavity unloaded Q

$$Q_0 = \frac{\omega_0 U}{P_l} = \frac{\omega_0 \mu_0}{R_S} \frac{\int |\mathbf{H}|^2 dV}{\int |\mathbf{H}|^2 dS}$$

$$\frac{Volume}{Surface} \approx a \approx \frac{c}{\omega_0}$$

Z_0 = 377 Ω

$$Q_0 = \frac{Z_0 f_{geometry}}{R_S}$$

Geometric factor

$$\boxed{G = Q_0 R_S}$$

Geometric factor depends only on cavity shape, and is independent of material, size or frequency. Typical G is about 270 Ω (the higher the better).

Lumped Circuit of an RF Cavity

Stored energy

$$U = \frac{1}{2}CV_c^2 = \frac{1}{2}LI^2$$

Power loss per cycle

$$P_c = \frac{V_c^2}{2R} = \frac{I^2R}{2}$$

Resonance frequency

$$\omega_0 = \frac{1}{\sqrt{LC}}$$

Cavity unloaded Q

$$Q_0 = \omega_0 RC$$

$$Q_0 = \frac{G}{R_S}$$

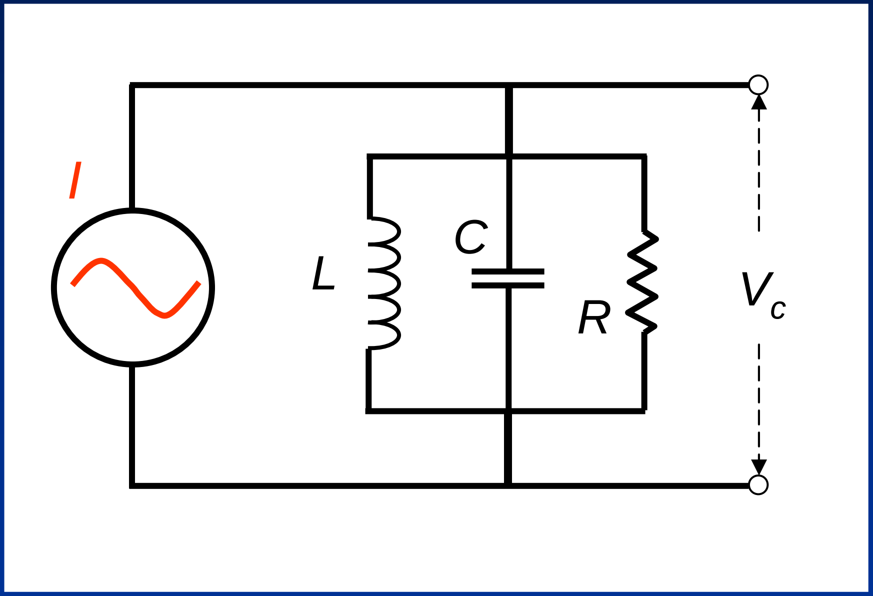

The cavity resonance frequency can be changed by adjusting its inductance or capacitance. Cavity inductance depends on the magnetic volume in the cavity. Capacitance depends on the spacing between the nose cones at the beam apertures. The unloaded Q scales linearly with shunt impedance, and inversely with surface resistance.

Shunt Impedance

Shunt impedance is a measure of how efficiently a cavity utilizes RF power toward accelerating the beam. The larger the shunt impedance, the higher the gradient at a fixed ohmic loss (or the lower ohmic loss for a given gradient). Shunt impedance per unit length (MΩ/m) is equal to the square of gradient (MV/m) divided by the ohmic loss (MW).

Shunt impedance per unit structure length

$$\boxed{r = \frac{R}{L} = \frac{E_0^2 L}{P_c}}$$

Transit-time corrected shunt impedance

$$\boxed{ZT^2 = \frac{\left(E_0 T\right)^2 L}{P_c}}$$

We can also calculate the RF power usage from the beam energy and accelerator length

$$\boxed{P_c = \frac{E_b^2}{\left(ZT^2\right) L}}$$

For copper linac, the shunt impedance per unit length depends on square root of frequency

$$\boxed{ZT^2 = \left(1.28\frac{M\Omega}{m}\right)\sqrt{\frac{f}{MHz}}}$$

R/Q

R/Q is a frequency- and material-independent geometric factor

$$\boxed{\frac{R}{Q} = \frac{V_c^2}{\omega_0 U}}$$

$$\propto a^2 \propto \frac{1}{\omega_0^2}$$

$$\propto a^3 \propto \frac{1}{\omega_0^3}$$

Pillbox TM_{010} R/Q = 196 Ω

Elliptical TM_{010} R/Q ~ 120 Ω

For the fundamental TM_{010} mode, large R/Q is good (low RF consumption for the same material). One can increase R/Q by changing the cavity from pillbox shape to re-entrant shape.

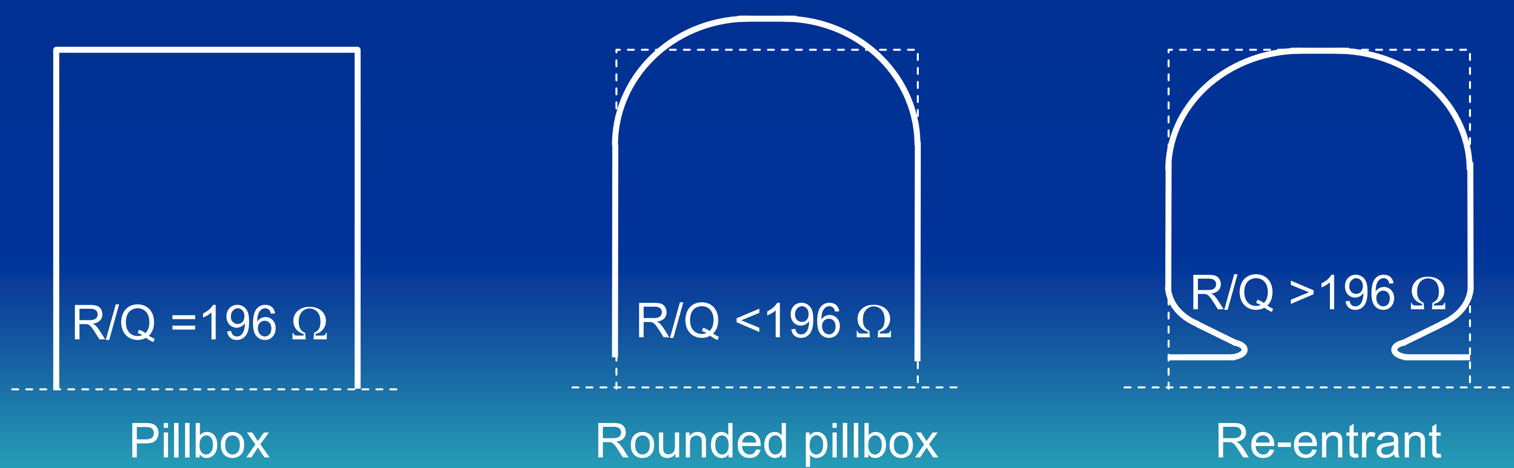

Coupled Cavity Linac (CCL)

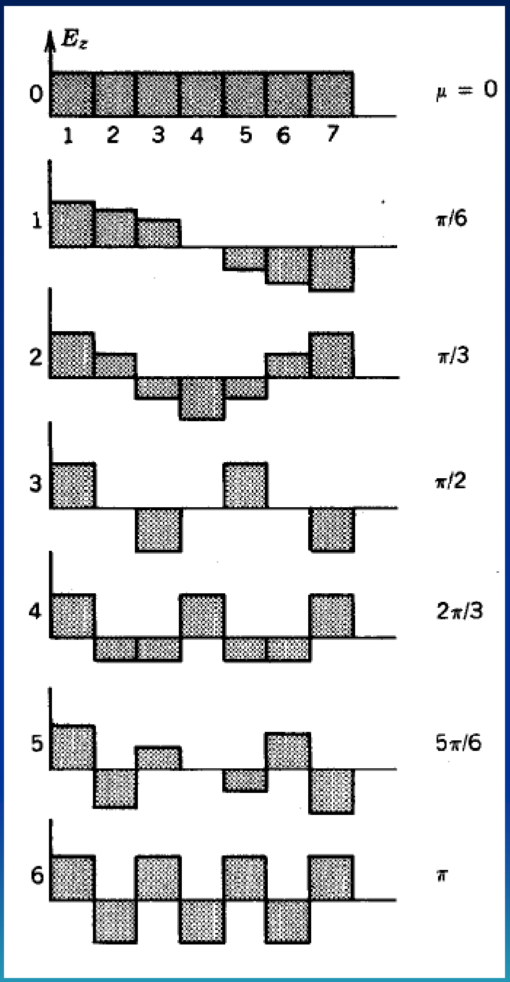

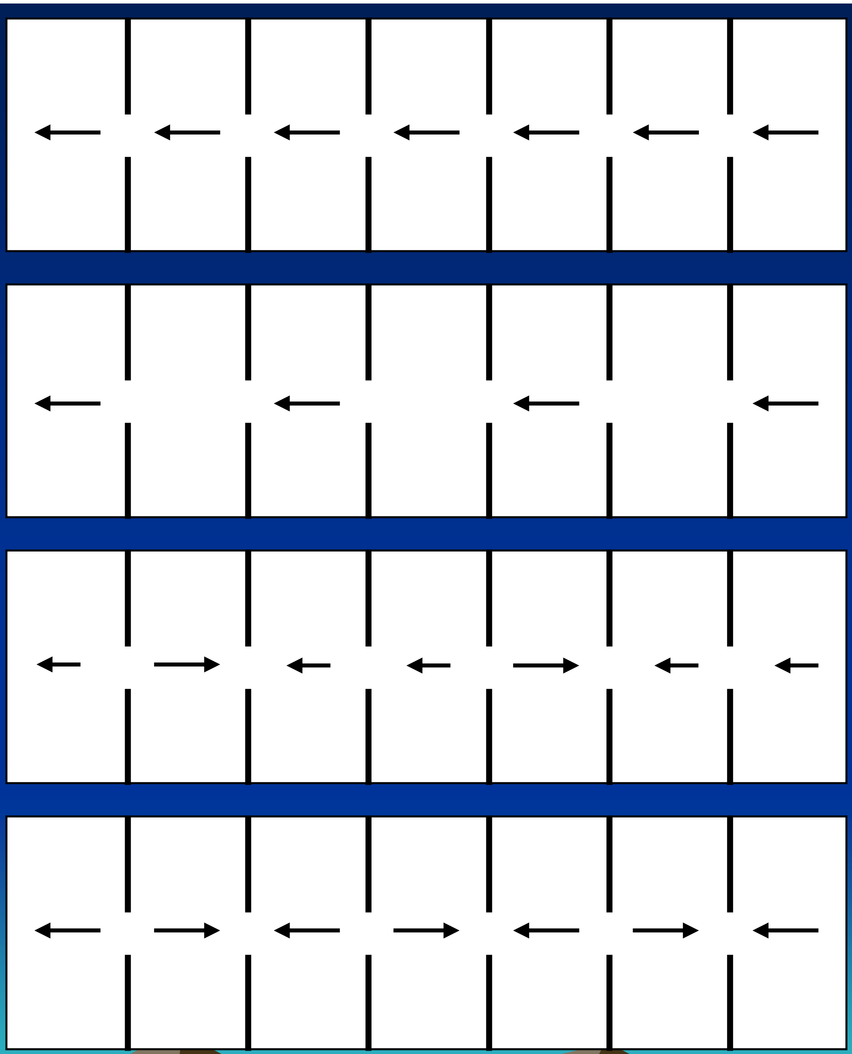

0 mode

π/2 mode

2π/3 mode

π mode

Cell-to-Cell Coupling

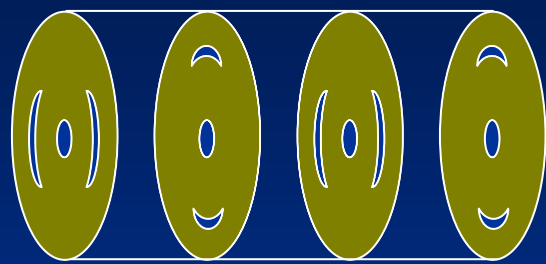

Magnetically coupled cavities

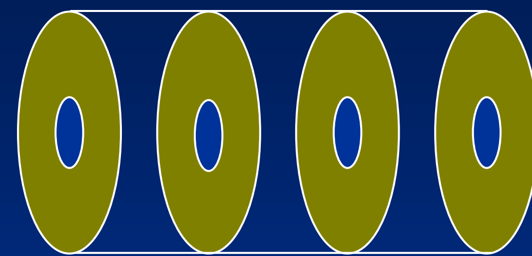

Electrically coupled cavities

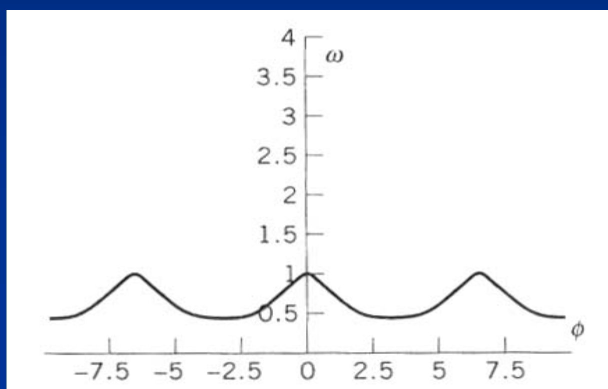

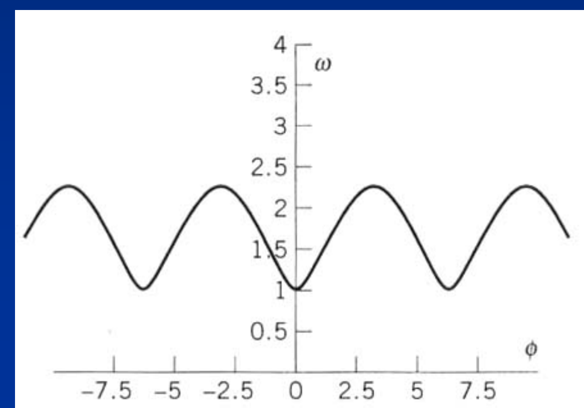

Coupled cavity linac is characterized by the phase advance from cell to cell. Typical phase advances for standing wave cavities are 0, $\pi/2$ and π. The 0 mode has the highest frequency in magnetically coupled CCL while the π mode has the highest frequency in electrically coupled CCL.

Dispersion Diagram for CCL

Frequency of CCL modes

$$\omega = \frac{2.405c}{a}\left[1 + \frac{\kappa}{2}\left(1 + \cos\psi\right)\right]$$

κ = cell-to-cell coupling

ψ = phase advance

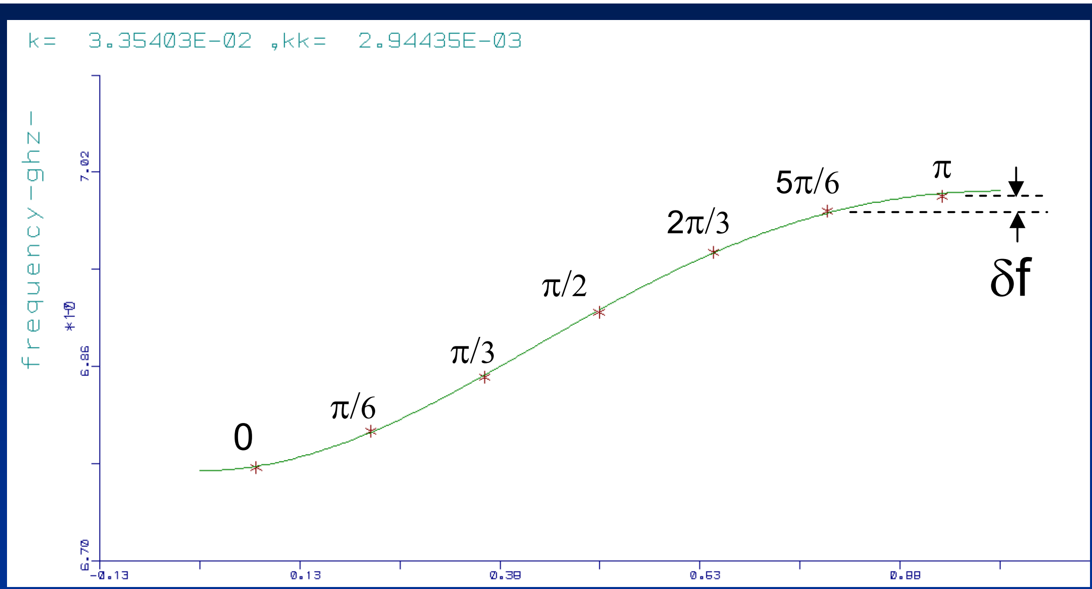

Dispersion diagram for CCL plots the mode frequency as a function of phase advance. For this CCL, the π mode is separated from the next mode by δf. To avoid field distortion due to mixing of nearby modes, the mode separation δf must be large compared to the bandwidth of the RF source.

Frequency separation between adjacent modes

$$\frac{\delta f}{f_0} \approx \frac{\kappa}{n}$$

Strong cell-to-cell coupling (large κ) means large frequency separation between modes, hence stable operation.

Transit Time

Transit time factor is defined as the ratio of voltage gain of an RF cavity relative to a DC cavity. Transit time factor is due to the sinusoidal variation of electric field during the electron transit through the cavity. To increase the transit time factor, one has to decrease the gap *d* between the cavity walls. This is often done by adding nose cones to NCRF cavities.

Transit time factor

$$T = \frac{\int_{-L/2}^{L/2} E_0 \cos(\omega t)\, dz}{\int_{-L/2}^{L/2} E_0\, dz}$$

RF voltage gain

DC voltage gain

$$T = \frac{\sin\left(\frac{\omega L}{2c}\right)}{\left(\frac{\omega L}{2c}\right)}$$

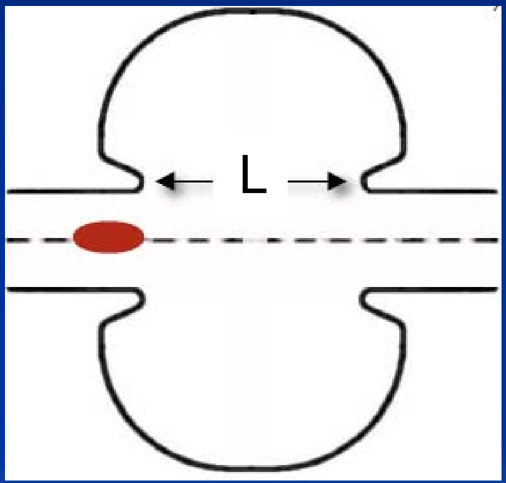

Maximum energy gain occurs at L = $\lambda_{RF}/2$ $\longrightarrow$ $T_{max} = \frac{2}{\pi}$

Energy Gain

The energy gain for the electrons in a TM_{010} electric field depends on the injection phase, defined such that $\phi = 0$ corresponds to maximum accelerating field (on crest).

Energy gain for particles with phase ϕ

$$\Delta W = -e \int_{-L/2}^{L/2} E_0 \cos(\omega t + \phi)\, dz$$

$$\Delta W = -e \int_{-L/2}^{L/2} E_0 \left[\cos\left(\frac{\omega z}{v}\right)\cos\phi - \sin\left(\frac{\omega z}{v}\right)\sin\phi\right] dz$$

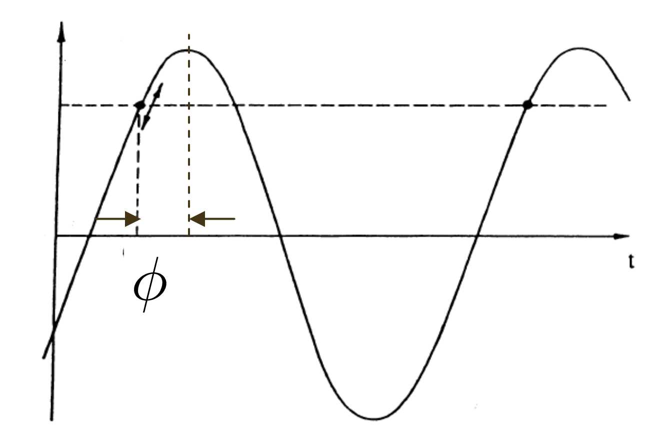

The second term is an odd function of z, so it integrates to zero. The first term integrates to

$$\Delta W = -eE_0 L \underbrace{\frac{\sin\left(\frac{\omega L}{2v}\right)}{\left(\frac{\omega L}{2v}\right)}}_{\text{Transit time factor}} \cos\phi \longrightarrow$$

Panofsky equation (for electrons)

$$\boxed{\Delta W = -eE_0 TL\cos\phi}$$

E_0T is the effective accelerator gradient, E_{acc}

Los Alamos NATIONAL LABORATORY EST. 1943

Accelerating Gradients

- Spatial average axial electric field: E_0

$$\mathbf{E} = E_0 e^{i\omega t + \vartheta_0}$$

- Average structure accelerating gradient, E_{acc}

$$E_{acc} = E_0 T$$

- Packing factor: length of active structure/total length

$$f_p = \frac{L_{acc}}{L_{total}}$$

- Real-estate gradient

$$E_{real} = E_{acc} f_p$$

For pulsed NCRF cavities at 3 GHz, the peak on-axis accelerating gradient is typically 50 MV/m. The average (transit time = 0.7) gradient is about 30 MV/m. Typical packing factor is 0.7 so real-estate gradient is ~ 20 MV/m.

For cw SRF cavities at 1.3 GHz, peak on-axis accelerating gradient is about 35 MV/m. The average (transit-time corrected) gradient is ~ 20 MV/m. Typical packing factor is 0.5, so the real-estate gradient is about 10 MV/m.

Power Loss per Cavity

$$P_l = \frac{R_s V_c^2}{G\left(\frac{R}{Q}\right)}$$

Normal-conducting Pillbox

- Surface resistance

$$R_s = 10m\Omega\sqrt{\frac{f}{1.5GHz}}$$

- G (= QR_s) is 257 Ω
- Q_0 ~ 25,000
- R/Q is ~200 Ω
- r ~ 50 MΩ/m
- P_c at 1 MV/m is 20 kW/m

Superconducting Elliptical

- Surface resistance

$$R_s = 8n\Omega + 10n\Omega\left(\frac{f}{1.5GHz}\right)^2$$

- G (= QR_s) is about 270 Ω
- Q_0 ~ 2 x 10^{10}
- R/Q is about 120 Ω
- r/Q ~ 600 Ω/m
- P_c at 1 MV/cell is ~10 W/m

RF Coupling

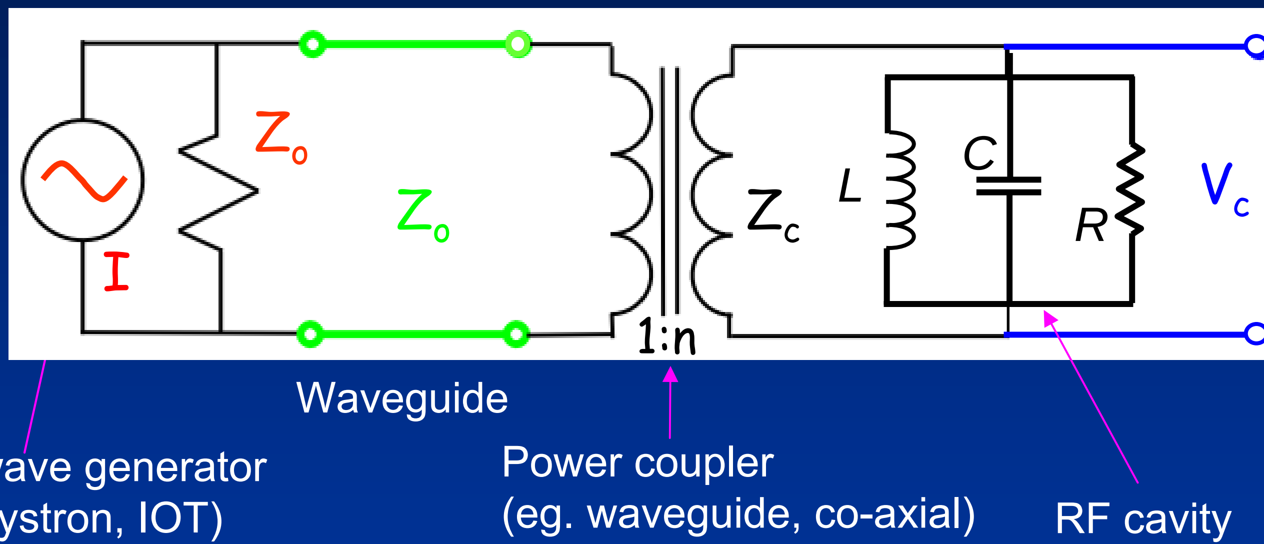

The microwave generator is typically connected to a circulator (not shown) and rectangular waveguides that transfer RF power to the cavity via a power coupler. A power coupler is used to match the waveguide impedance into the cavity impedance. If the impedance is not matched, RF power will be reflected back to the circulator. The circulator then directs the reflected power to a matched load (protecting the generator from seeing the reflected power).

External Q

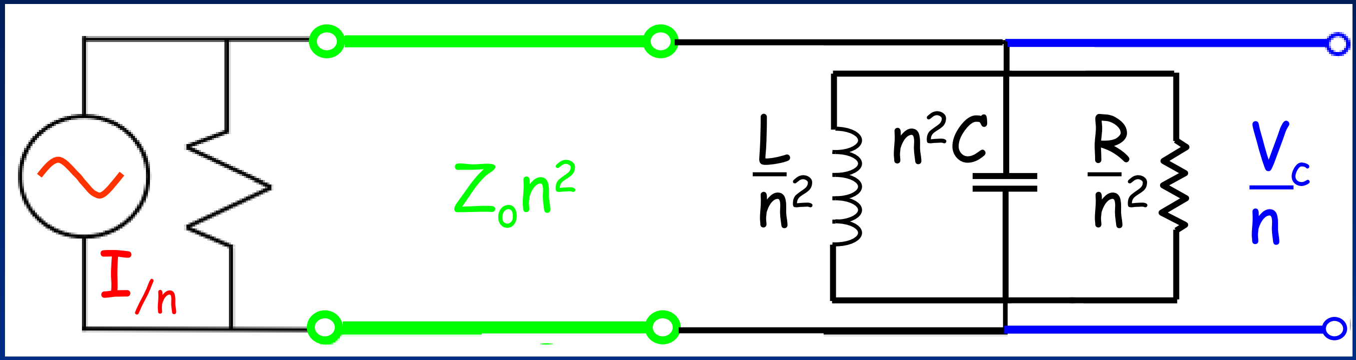

Cavity impedance as seen by the waveguide

$$Z'_c = \frac{Z_c}{n^2}$$

Stored energy

$$U = \frac{n^2}{2} C V_c^2$$

External power

$$P_{ext} = \frac{1}{2Z_0}\left(\frac{V_c}{n}\right)^2$$

External Q

$$Q_{ext} = \omega_0 n^2 Z_0 C$$

Loaded Q

$$\frac{1}{Q_L} = \frac{1}{Q_0} + \frac{1}{Q_{ext}}$$

Typical unloaded Q is 10^{10} and external Q is about 10^6

Coupling Beta with No Beam

Coupling β $$\beta = \frac{P_{ext}}{P_c} = \frac{Q_0}{Q_{ext}}$$

β < 1 Undercoupled

β = 1 Critically coupled

β > 1 Overcoupled

Reflected power

$$P_- = \left|\frac{\beta - 1}{\beta + 1}\right|^2 P_+$$

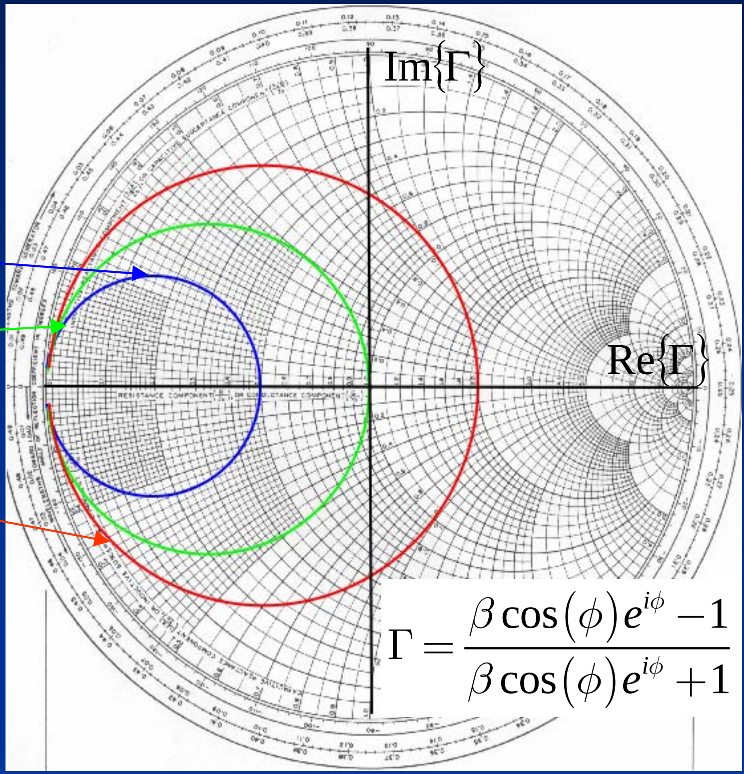

$$\Gamma = \frac{\beta\cos(\phi)e^{i\phi} - 1}{\beta\cos(\phi)e^{i\phi} + 1}$$

Cavity power

$$P_c = \frac{4\beta}{(1+\beta)^2} P_+$$

Reflected power is zero at β=1 (critical coupling)
Max. cavity power at β=1 is equal to forward power.

Lumped Circuit of Cavity with Beam

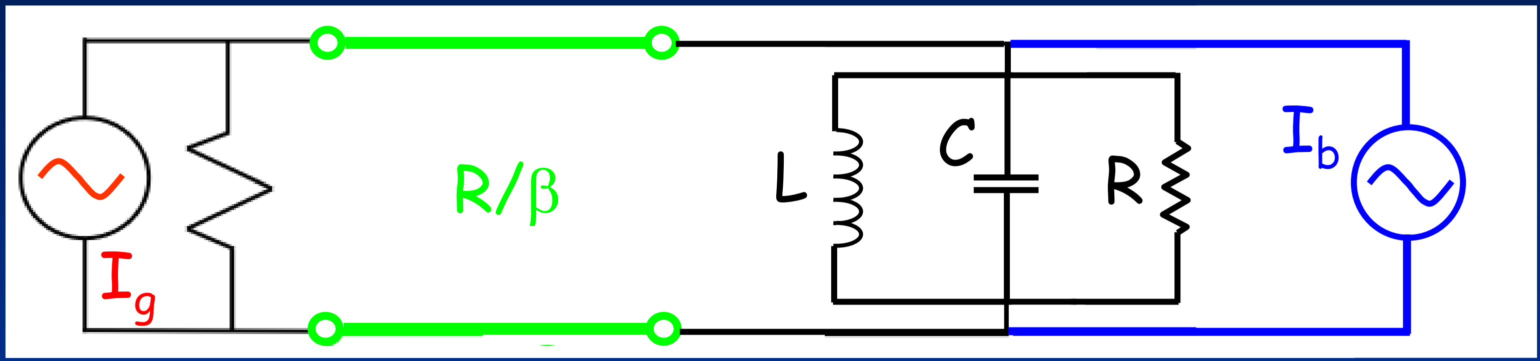

Beam Voltage

$$V_b = -I_b R$$

Beam Power

$$P_b = IV_c \cos\phi$$

Loaded Q

$$\boxed{\frac{1}{Q_L} = \frac{1}{Q_0} + \frac{1}{Q_{ext}} + \frac{1}{Q_b}}$$

Voltage Phasor Diagram

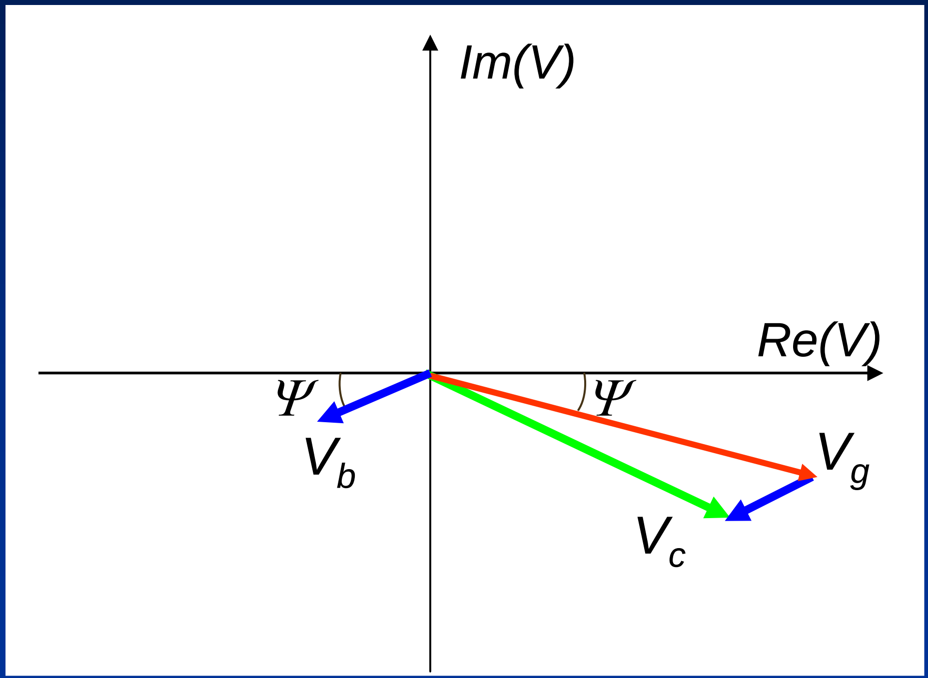

If electrons are injected off-crest, the cavity resonant frequency is not exactly the driving frequency. The detuning angle is given by

$$\tan\Psi = -2Q_L \frac{\Delta\omega}{\omega_0}$$

Generator voltage

$$V_g = V_c + V_b$$

Coupling Beta with Beam Loading

Matched coupling beta

$$\beta_0 = 1 + \frac{P_b}{P_c}$$

Loaded Q

$$Q_L = \frac{Q_0}{1+\beta_0}$$

Total power

$$P_{gen} = P_c + P_b + P_{ref}$$

Reflected power

$$P_- = \left|\frac{\beta-\beta_0}{\beta+\beta_0}\right|^2 P_+$$

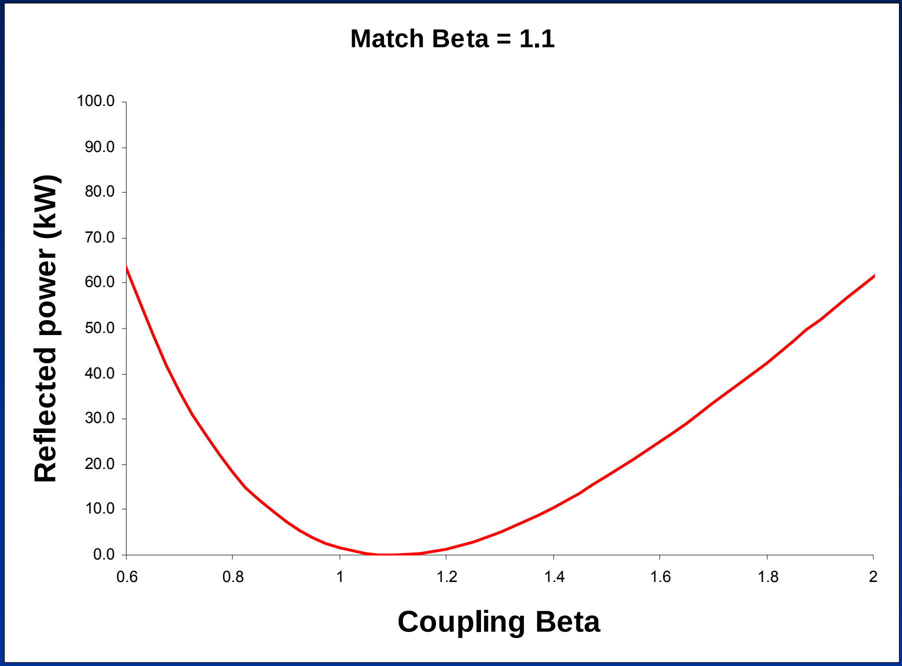

Reflected power is minimized by “matching” the coupling beta to the cavity coupling with beam. Note the cavity is “matched” only at one beam power (beam current).

Heavy Beam-Load Phasor Diagram

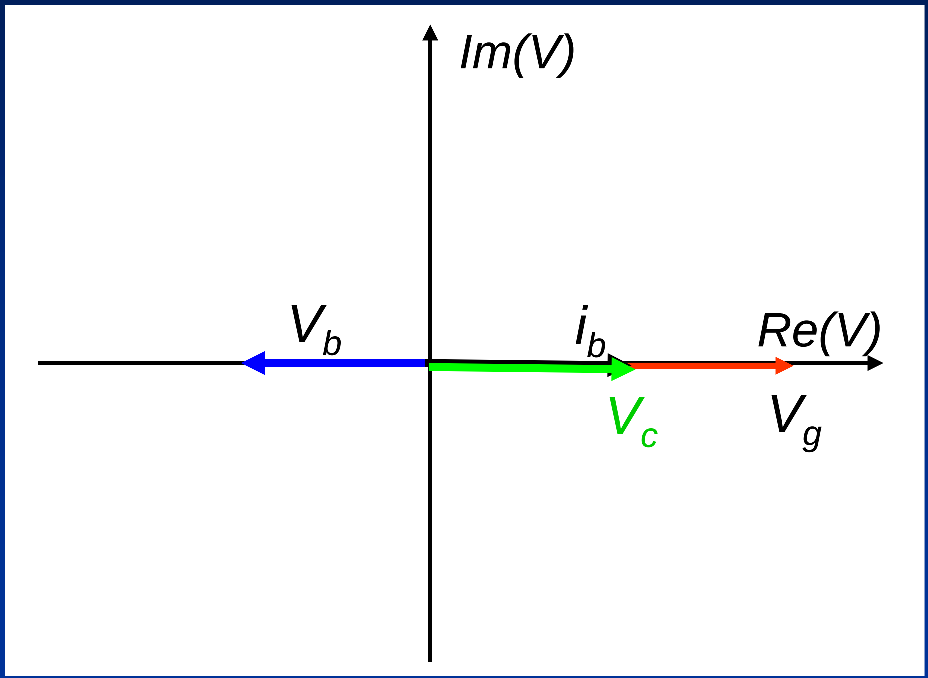

Generator voltage

$$V_g = V_c + V_b = 2V_b$$

Generator power

$$P_g = 4P_b$$

References

Books

Science and Technology of Undulators and Wigglers	J.A. Clark
RF Linear Accelerators	T.P. Wangler
RF Superconductivity for Accelerators	H. Padamsee

URL

http://www.slac.stanford.edu/cgi-wrap/getdoc/slac-pub-8026.pdf

http://srf2003.desy.de/talks/Knobloch/Knobloch_tutorial_srf_2003.pdf

http://en.wikipedia.org/wiki/Superconducting_Radio_Frequency